Marine and Petroleum Geology 99 (2019) 1–16

Contents lists available at ScienceDirect

Marine and Petroleum Geology

journal homepage: www.elsevier.com/locate/marpetgeo

Research paper

Factors controlling reservoir properties and hydrocarbon accumulation of the Eocene lacustrine beach-bar sandstones in the Dongying Depression, Bohai Bay Basin, China

Jian Wang[a,b,*], Yingchang Cao[a,b,**], Jie Xiao[a], Keyu Liu[a,c], Mingshui Song[d]

[a] School of Geosciences, China University of Petroleum (East China), Qingdao, 266580, China
[b] Laboratory for Marine Mineral Resources, Qingdao National Laboratory for Marine Science and Technology, Qingdao, 266071, China
[c] Department of Applied Geology, Curtin University, GPO Box U1987, Perth, WA, 6845, Australia
[d] Institute of the Shengli Oilfield, SINOPEC, Dongying 257015, China

ARTICLE INFO

Keywords:
Reservoir petrophysical property
Diagenesis
Compaction
Carbonate cementation
Hydrocarbon accumulation
Dongying depression

ABSTRACT

Lacustrine beach-bar sandstone reservoirs are economical important exploration targets in the Dongying Depression, Bohai Bay Basin. The factors that controls reservoir quality and hydrocarbon accumulation in lacustrine beach-bar sandstones were systematically investigated through an integrated petrographic, petrophysical, and diagenesis analysis. The reservoir properties of the beach-bar sandstones are mainly affected by compaction, carbonate cementation and dissolution. Significant negative relationships exist between both the porosity and permeability and the volume of carbonate cement. Carbonate cement is mainly distributed along the sandstone-mudstone contacts. Sandstones with thicknesses less than 1 m are generally tightly cemented to form zones with low petrophysical properties. The material source of the carbonate cement in the tightly cemented zone was highly likely from the interbedded mudstone. Content of carbonate cements in the center of the thick sandstones is low, whereas compaction is the dominant diagenetic process, with some dissolution. There is a positive correlation between the petrophysical properties of the beach-bar sandstones and the content of kaolinite. The petrophysical properties have an inverse correlation with the contents of illite and illite-smectite mixed-layer clays. Reservoir petrophysical property largely controls hydrocarbon accumulation in the beach-bar sandstones. Compared with non-oil bearing sandstones, oil-bearing sandstones have higher porosity and a larger pore-throat size. Sandstones with a porosity of less than 8.5% and/or low permeability of less than 1.02×10^{-3} μm^2 are mostly incapable of accumulating oil.

1. Introduction

The term 'beach-bar' is a comprehensive term that describes the beach and the bar sandbodies in the shallow-water zones of lacustrine basins (Monroe, 1981; Reid and Frostick, 1985; Basilici, 1997; Patel et al., 2002; Deng et al., 2011; Jiang et al., 2011). Terrigenous clastic beach-bar sandbodies usually develop in open littoral and shallow lakes, which are formed from the re-handling and re-deposition of shallow water deltas (Deng et al., 2011; Gao et al., 2014) and other associated near-shore shallow sedimentary systems under the action of waves and coastal currents (Cao et al., 2010; Deng et al., 2011; Jiang et al., 2011; Goulart and Calliari, 2013; Gao et al., 2014). In the Bohai Bay Basin, Beach-bar sandstone reservoirs occur in a many kinds of tectonic settings, such as rift lacustrine basins, depression lacustrine basins, intracratonic lacustrine basins and foreland lacustrine basins, and greatly affect the geometries and characteristics of reservoirs (Williams et al., 1975; Aitken et al., 1988; Engels and Roberts, 2005; Fisher, 2005; Jiang et al., 2011; Zhao et al., 2014). There are large scale of lacustrine beach-bar sandstone reservoirs in the Eocene depressions in the Bohai Bay Basin (Fig. 1A; Deng et al., 2011; Jiang et al., 2011; Gao et al., 2014), e.g., during deposition of the Es4s, beach-bar sandbodies covered ca 50%–70% of the Boxing Sag, ca 660–924 km^2 (Jiang et al., 2011), which provides a good opportunity to thorough understand the characteristics of lacustrine beach-bar reservoirs because of its representativeness and relatively rich data (Cao et al., 2010; Jiang et al., 2011).

With the increase of the hydrocarbon exploration activities in the Dongying Depression, the focus of the exploration has gradually

* Corresponding author. School of Geosciences, China University of Petroleum, Qingdao, Shandong 266580, China.
** Corresponding author. School of Geosciences, China University of Petroleum (East China), Qingdao 266580, China.
E-mail addresses: wangjian8601@163.com, caoych@upc.edu.cn (J. Wang), caoych@upc.edu.cn (Y. Cao).

https://doi.org/10.1016/j.marpetgeo.2018.09.022
Received 9 April 2018; Received in revised form 20 June 2018; Accepted 17 September 2018
Available online 27 September 2018

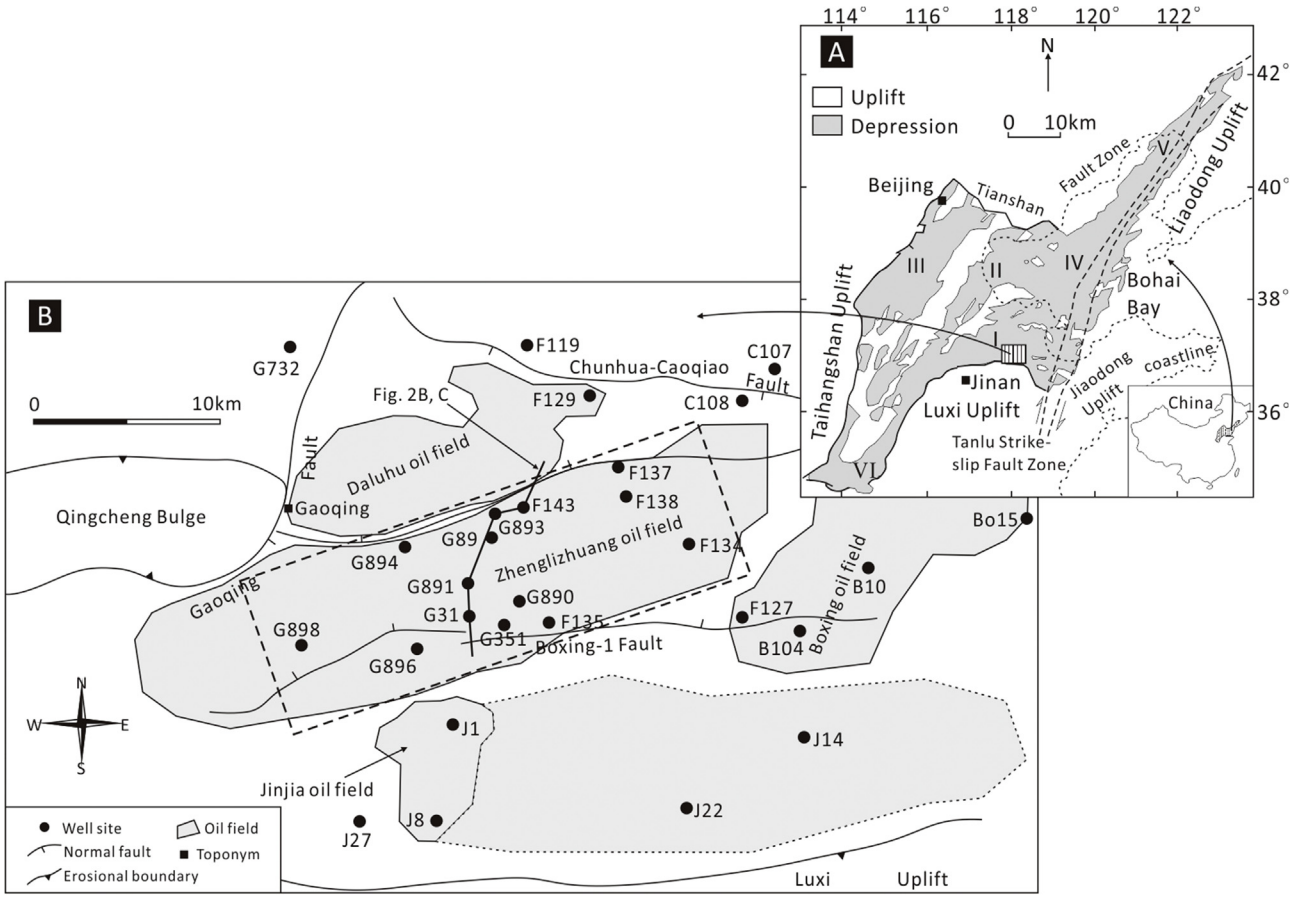

Fig. 1. (A) Tectonic setting of the Boxing Sag in the southern Jiyang subbasin (I) of the Bohai Bay Basin. Other subbasins in the Bohai Bay Basin include the Huanghua subbasin (II), Jizhong subbasin (III), Linqing subbasin (IV), Bozhong subbasin (V) and Liaohe subbasin (VI). (B) Structural map of the Boxing sag with the well locations and the main faults in the Es4s unit.

transferred from high-permeability to low-permeability sandstones and from structural to stratigraphic traps (Yuan and Qiao, 2002; Li et al., 2014). In recent years, beach-bar plays have become one of the main exploration targets in the Dongying Depression (Zhang et al., 2005). Since 2005, six oil fields, namely, the Jinjia, Zhenglizhuang, Daluhu, Boxing, Chuanhua-Xiaoying and Wangjiagang oil fields, have been found in beach-bar reservoirs in the upper fourth member of the Eocene Shahejie Formation (Es4s) in the Dongying Depression (Fig. 2), which show the enormous exploration potential of the beach-bar sandbodies in this area. Exploration has shown that the Eocene beach-bar sandstone reservoir is a typical low-permeability (permeability of more than 90% of the samples is less than 10×10^{-3} μm^2) reservoir with medium-low porosity (porosity of more than 85% of the samples is less than 15%), complicated pore-throat structure, strong heterogeneity and low recovery (Han, 2009; Tian and Jiang, 2012). Considerable studies have been performed on the beach-bar sandstone reservoirs over the past few years, but most of the research results were focused on their sedimentary characteristics and depositional models (Deng et al., 2011; Jiang et al., 2011; Tian and Jiang, 2012; Gao et al., 2014; Guo et al., 2014; Zhao et al., 2014). However, studies on the factors controlling reservoir properties and hydrocarbon accumulation in the lacustrine beach-bar sandstones are limited because of the characteristic of thin layer (usually 0.5–4.5 m), low permeability and complex diagenesis (Si et al., 2007; Wang et al., 2017b) Searching for high-quality reservoir with high abundance of oil enrichment is the key for the exploration and exploitation of low-permeability sandstone reservoirs. Therefore, a systematical study of the reservoir characteristics of beach-bar sandstones and the controlling factors on the reservoir quality and hydrocarbon accumulation was investigated through an integrated petrographic, petrophysical, and diagenesis analysis. The results of this study can help oil and gas exploration and exploitation in the lacustrine deposits in the Bohai Bay Basin and other similar basins, e.g., the Paleogene in the Subei Basin (Ji et al., 2013) and the Paleogene in the Pearl River Mouth Basin (Liu et al., 2015).

2. Geological background

The Bohai Bay Basin (Fig. 1A), which is an important hydrocarbon-producing basin (By the end of 2013, the proved petroleum reserves is 140.52×10^8t; production of oil and gas equivalent in 2013 was 7596×10^4t (Zhao et al., 2015)), is located on the eastern coast of China. The basin is a complex rifted basin formed in the Late Jurassic through the early Tertiary on the basement of the North China platform. The tectonic evolution of the basin consists of a synrift stage (65.0–24.6 Ma) and a postrift stage (24.6 Ma to the present) (Lampe et al., 2012). The Boxing Sag is a secondary tectonic unit of the Dongying Depression (Fig. 1A) bounding to the Gaoqing fault in the west, Shicun fault in the east, Chunhua-Caoqiao fault in the north and Luxi Uplift in the south (Fig. 1B). The Boxing-1 and Boxing-2 faults are 2 s-order faults in the center of the Boxing Sag (Jiang et al., 2011).

The Boxing Sag developed on a northward-dipping, subsiding, faulted block within the Dongying Depression (Jiang et al., 2011, Fig. 1B). The sag is filled with the Cenozoic to Quaternary deposits, which are composed of the Kongdian (Ek), Shahejie (Es), Dongying (Ed), Guantao (Ng), Minghuazhen (Nm) and Pingyuan (Qp) formations (Fig. 2A). The upper part of the fourth Member of the Shahejie Formation (Es4s) consists of fine-grained and thin-bedded sandstones interbedded with gray mudstone, which is the focus of this study. The

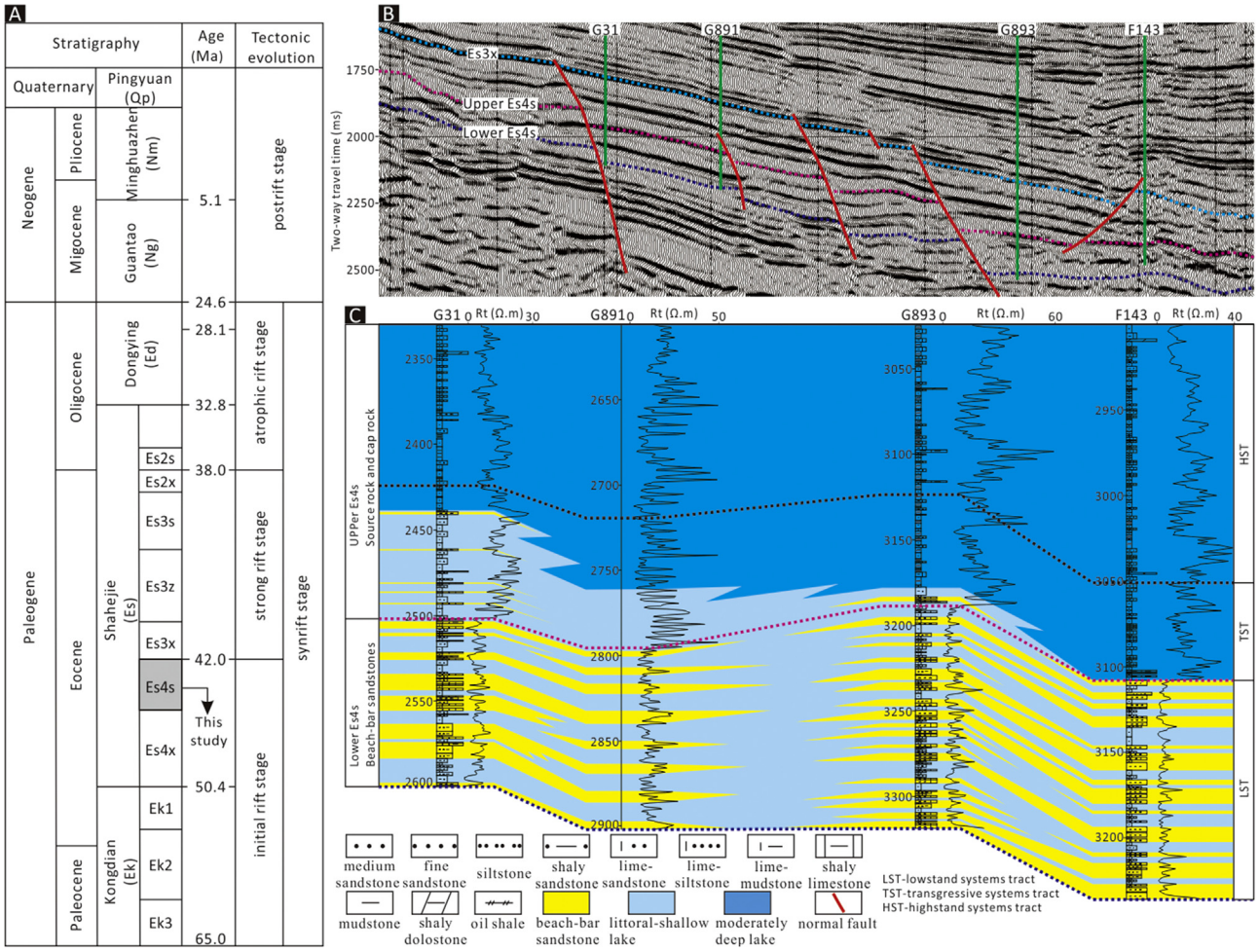

Fig. 2. (A) Schematic Tertiary stratigraphy and tectonic evolution of the Boxing Sag. The Es4s unit developed during the initial rift stage and comprises sandstones that are interbedded with mudstones. Beach-bar sandstones mainly occur in the lower part of the Es4s Member. (B) Seismic section cross Wells G31 to F143 showing the distribution of the upper and lower parts of the Es4s Member. (C) Sedimentary cross-section from Wells G31 to F143 along a north/south direction in the Boxing Sag. Qp-Quaternary Pingyuan Formation; Nm-Neocene Minghuazhen Formation; Ng-Neocene Guantao Formation; Ed1-the first Member of the Paleogene Dongying Formation (Ed); Ed2-the second Member of Ed; Ed3-the third Member of Ed; Es1-the first Member of the Paleogene Shehejie Formation (Es); Es2s-the upper second Member of Es; Es2x-the lower second Member of Es; Es3s-the upper third Member of Es; Es3z-the middle third Member of Es; Es3x-the lower third Member of Es; Es4s-the upper fourth Member of Es; Es4x-the lower fourth Member of Es; Ek1-the first member of the Paleogene Kongdian Formation. Systems tracts are after Jiang et al. (2011). See Fig. 1B for the location of seismic section and sedimentary cross-section.

Es4s member developed during the late period of the initial rift stage, and is divided into the lower part (Es4scx, avg. 140 m) and the upper part (Es4scs, avg. 160 m) according to the stratigraphic and rock characteristics (Fig. 2B and C). During the depositional stage of the Es4scx, large-scale shore-shallow beach-bar sandbodies developed under the conditions of gentle paleotopography (Fig. 2C, Jiang et al., 2011), semi-arid to semi-humid paleoclimate, high salinity lake water (Wang et al., 2015), a shore-shallow lacustrine environment and a relative abundance of sediment supply. During the sedimentary stage of the Es4scs, large-scale dark-gray mudstones and shale developed, which are some of the major hydrocarbon source rocks in the Boxing Sag (Fig. 2C, Guo et al., 2010; Guo et al., 2014).

The Zhenglizhuang oilfield is located in the southeastern part of Gaoqing County and lies between the Gaoqing oilfield and the Jinjia oilfield. The tectonic location of the Zhenglizhuang oilfield is mainly between the Boxing-1 and Boxing-2 faults (Fig. 1B), with more than 200 exploration wells and 13 cored wells. Analyses of drill, seismic and core data indicate that the beach-bar sandstones in the Zhenglizhuang oilfield trend NE-SW. The strata, which are characterized by sandstone and mudstone interval layers, are up to 200 m thick. The beach-bar sandstones are usually buried between the depths of 2200 and 3500 m.

3. Samples and methods

13 exploration wells with approximately 634 m cores were employed to collect samples of beach-bar sandstones in the study area (Fig. 1B). Samples were impregnated with blue resin before thin sectioning in order to highlight pores. Thin sections were partly stained with Alizarin Red S and K-ferricyanide for carbonate mineral determination. Point counting method was used to determine the composition, and 135 thin sections were analyzed by counting 300 points per thin section. The classification scheme for the beach-bar sandstone was based on Folk (1980). The Udden-Wentworth grain size scale was used to determine the sandstone grain size (Udden, 1914; Wentworth, 1922). According to the standard charts of Folk (1980) the sorting was determined. Ten samples were analyzed using a Hitachi S-4800 scanning electron microscopy under the conditions of 20 °C, 35%RH, 5.0 kV, and less than 15 mm WD. A total of 102 samples were collected for clay mineral analyses and 52 samples were collected for mudstone composition analyses using X-ray diffraction (XRD) through a D8 DISCOVER with Cu-Ka radiation, a voltage of 40 kV, and a current of 25 mA. Before the analyses, every sample was oven-dried at 40 °C for 2 days and in order to completely disperse the minerals, an agate mortar was used to ground these samples to less than 40 mm without chemical pre-

treatment. In order to analyze the compositions of clay minerals, the samples were put in a plastic bottle, soaked in distilled water, and then disintegrated with an oscillator. Distilled water was added to the sample until the conductivity is less than 50 μs/cm, and the suspension was separated by a centrifuge at a speed of 2000 r/min for 2 min. Filtering granular suspension less than 2 μm with ceramic filter, and then the clay mineral particles were placed in an oven to dry at 50 °C. Samples were scanned from 3° to 70° with a step size of 0.02°. The relative content of the multiple clay mineral phases in weight percent was identified through diffractograms and semiquantitatively analyzed by computer analyses.

528 cylinders drilled from the cores with diameters of 2.5 cm were used to determine the porosity and permeability. The porosity was measured following Boyle's law via using a helium porosimeter. The preprocessed sample (dry, clean) was injected with helium at approximately 200 psi in a porosimeter. The grain volume was calculated by measuring the corresponding pressures and volumes through the Boyle's Law equation. The bulk volume that was measured through the Archimedes Principle with mercury immersion was used to determine the pore volume by subtracting the grain volume, and then the grain and bulk volumes were used to calculate total porosity. The permeability was measured following Darcy's law using a gas permeameter. The preprocessed sample was injected with dry air under approximately 980Pa differential pressure to ensure that the air passes through the filter plate under the laminar flow condition.

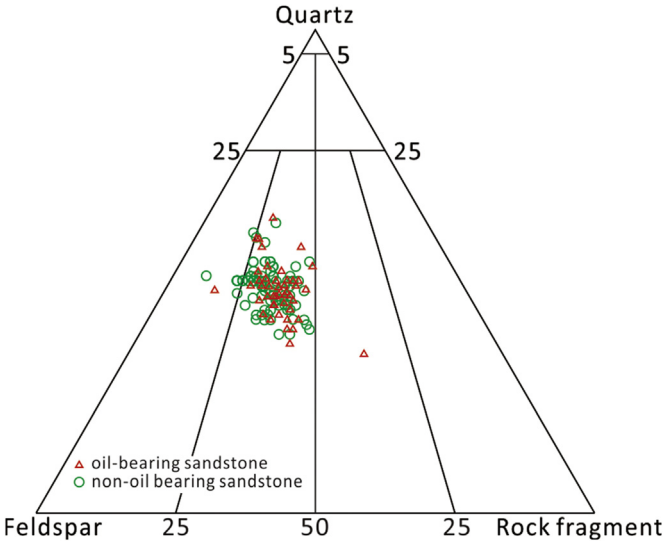

Fig. 3. Detrital composition triangular diagram of the oil-bearing and non-oil-bearing beach-bar sandstones in the Boxing Sag. The samples mainly plot in the lithic arkose field and rarely in the arkose and feldspathic litharenite fields based on the classification of Folk (1980).

4. Results

4.1. Petrological characteristics of sandstones

Compositions of oil-bearing and non-oil bearing beach-bar sandstones are summarized in Table 1. The detrital compositions of oil-bearing sandstones and non-oil bearing sandstones are mainly lithic arkoses according to Folk (1980) classification scheme, with corresponding average compositions for the two types of sandstones being $Q_{43.2}F_{30.5}R_{26}$, $Q_{42.2}F_{35.3}R_{22.3}$ (Fig. 3). There is no obvious difference in the content of detrital quartz between oil-bearing and non-oil bearing sandstones (Table 1). The contents of potassium feldspar and plagioclase feldspar in oil-bearing sandstones are lower than those in non-oil bearing sandstones (Table 1). Lithic fragments are mainly of volcanic and metamorphic types, which are higher in oil-bearing sandstones. Other detrital components include mainly small amounts of mica and chert (Table 1). The average grain sizes of the beach-bar sandstones are mainly between 0.04 mm and 0.16 mm, of which 62.3% of the samples are 0.0625–0.125 mm (very fine sand) and 23% of the samples are 0.125–0.25 mm (fine sand). The sorting coefficient of the beach-bar sandstones is between 1.28 and 4.63, with an average of 1.77, indicating medium to good sorting for most of the sandstones. The roundness of almost all the detrital particles of the beach-bar sandstones in the Zhenglizhuang oilfield are hypo-edge angle (Fig. 4).

Table 1
The compositions and differences of the oil-bearing and non-oil bearing beach-bar sandstones in the Boxing Sag.

	Oil-bearing sandstones			Non-oil bearing sandstones		
	Min	Max	Mean	Min	Max	Mean
Detrital grains						
Quartz (vol. %)	24.1	53.5	43.2	24.4	53.5	42.2
Potassium feldspars (vol. %)	8.4	22.3	15.4	9.1	25.6	17.8
Plagioclase feldspars (vol. %)	8.8	27.9	15.1	9.4	30.2	17.5
Volcanic lithic fragments (vol. %)	1.9	45.1	15.3	1.3	45.7	12.2
Metamorphic lithic fragments (vol. %)	5.1	19.2	9.3	5.1	19.6	8.5
Sedimentary lithic fragments (vol. %)	0	15.3	1.4	0	16.7	1.6
Mica (vol. %)	0	2.2	0.1	0	2.5	0.1
Chert (vol. %)	0	2.1	0.2	0	2.3	0.1
Matrix (vol. %)	0	23.3	7.8	0	25.4	7.5
Diagenetic alterations						
Calcite (vol. %)	0.5	13.3	4.5	8	30.2	14.2
Dolomite (vol. %)	0	6.2	1.5	0.5	17.4	3.1
Ankerite (vol. %)	0	2.3	1.1	0	1.5	0.7
Quartz overgrowths (vol. %)	0.4	3.5	1.2	0	2.5	0.4
Pyrite (vol. %)	0.5	5.6	0.3	0	3.5	0.2
Clay minerals (vol. %)	2	10	5	0	18	5.6
Kaolinite (%)	8	38	29.4	1	30	20.1
Illite (%)	25	52	38.9	30	71	46.5
Illite-smectite mixed layer clays (%)	3	45	25.3	6	53	26.1
Chlorite (%)	1	18	6.4	2	20	7.3
Porosity						
Intergranular porosity (vol. %)	4.5	17.2	6.6	0	6.3	1.2
Intragranular porosity (vol. %)	0.5	2.8	0.9	0	0.7	0.1

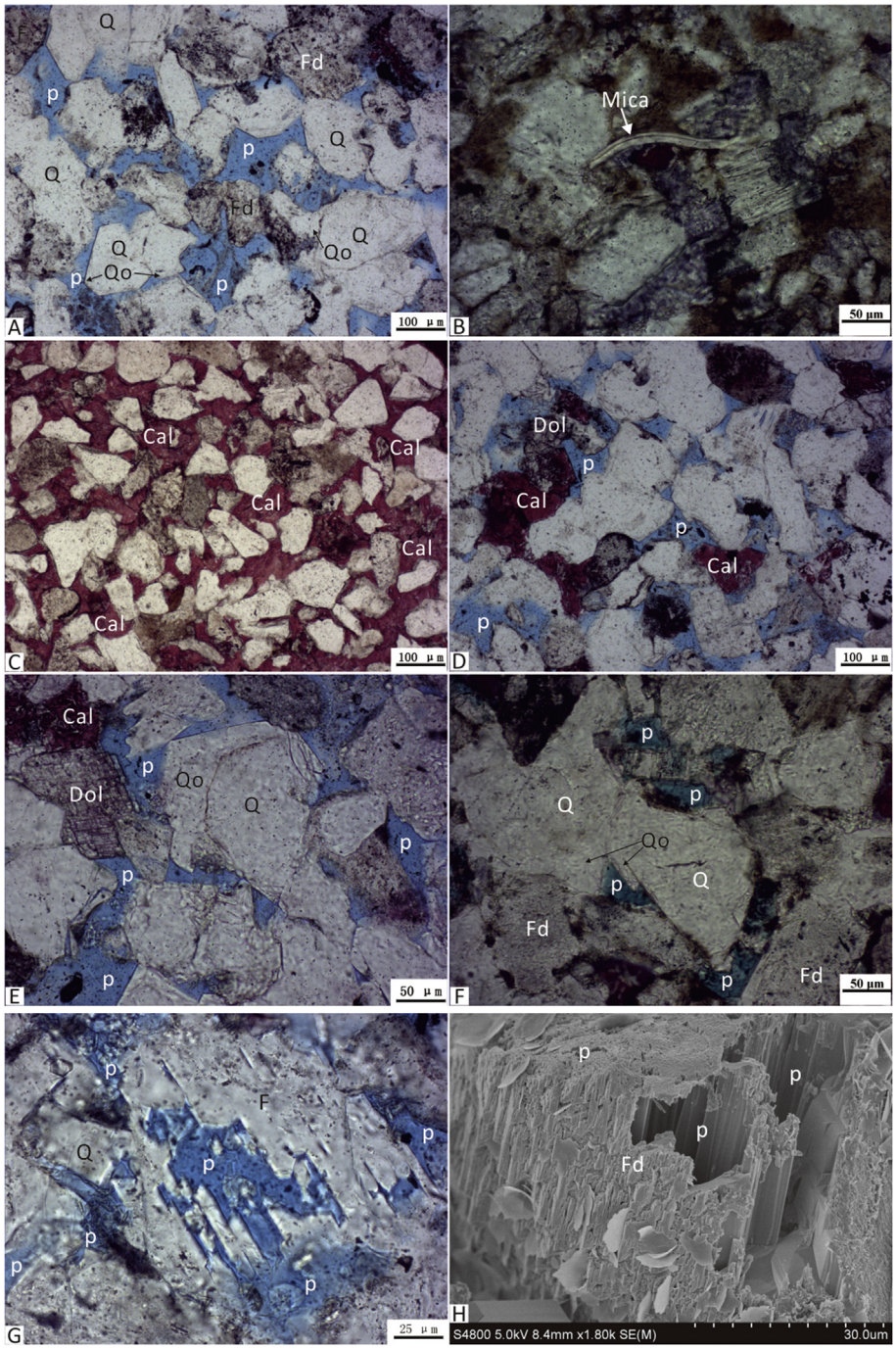

Fig. 4. (A) Point-line contact between detrital grains, primary intergranular pores and quartz overgrowth from well G890 at 2598.2 m (PPL); (B) Deformation of micas and line-concavo-convex contact between detrital grains from well F137 at 3169.7 m (PPL); (C) Crystalline calcite filling in intergranular pores, point contact between detrital grains from well G351 at 2446.19 m (PPL); (D) Isolated calcite and dolomite and intergranular pores from well G890 at 2598.2 m (PPL); (E) Isolated calcite and dolomite, quartz overgrowth, and intergranular pores from well G351 at 2434.24 m (PPL); (F) Quartz overgrowth and intergranular pores from well F137 at 3171.6 m (PPL); (G) Feldspar dissolution pores and intergranular pores from well G890 at 2599.7 m (PPL); (H) Feldspar dissolution pores from well F151-1 at 2701 m (PPL). P-pore, Q-quartz, Fd-feldspar, Cal-calcite, Dol-dolomite, Qo-quartz overgrowth, (PPL) indicates the plane polarized light.

4.2. Petrological characteristics of mudstones

The XRD compositions of mudstones interbedded with beach-bar sandstones are summarized in Table 2. Quartz, feldspar and clay minerals are the most abundant components in mudstones interbedded with beach-bar sandstones. Content of K-feldspar is obviously lower than that of Plagioclase feldspar. Carbonates in mudstones are dominated by calcite and ankerite. Clay minerals are dominated by illite-smectite mixed layer clays and illite.

4.3. Diagenesis and authigenic minerals in sandstones

The reservoir petrophysical properties and thin section analysis indicate that the Eocene beach-bar sandstones experienced complex diagenetic processes. The diagenesis that controlled the beach-bar reservoir quality mainly included compaction, carbonate cementation, quartz overgrowth cementation, clay mineral cementation and the dissolution of unstable components.

(1) Compaction: Evidence of the compaction of the beach-bar sandstone reservoirs is significant in the burial depth range of 2200–3500 m. The contact types are changed from point contacts and line contacts to concavo-convex contacts or line-concavo-convex contacts with increasing burial depth (Fig. 4A and B), which are dominated by point and line contacts. Ductile grains such as mica are commonly deformed (Fig. 4B).
(2) Carbonate cements: The interstitial matter in the beach-bar sandstone reservoirs comprises carbonate cements, authigenic quartz and clay matrix (Table 1). Carbonate cements are the most common authigenic minerals in the beach-bar sandstones, which usually fill

Table 2
The compositions of the mudstones interbedded with beach-bar sandstones in the Boxing Sag.

	Min	Max	Mean
Quartz (wt. %)	20	33	27.8
Potassium feldspars (wt. %)	3	15	5.3
Plagioclase feldspars (wt. %)	8	21	14.1
Calcite (wt. %)	7	16	12.7
Dolomite (wt. %)	0	4	1.7
Ankerite (wt. %)	0	20	5.1
Clay (wt. %)	11	53	32.4
Kaolinite (wt. %)	0	9	3.8
Illite-smectite mixed layer clays (wt. %)	33	80	55.7
Illite (wt. %)	16	65	33.3
Chlorite (wt. %)	2	16	5.3
Pyrite (wt. %)	0	3	1.1

primary intergranular pores or feldspar dissolution pores (Fig. 4C, D, E and Fig. 5C, D, E, F). Carbonate cement mainly consists of calcite, dolomite and ankerite, of which calcite is the main type. There are two types of calcite cements in beach-bar sandstone reservoirs. The first type fills all the intergranular pores as crystalline calcite cements. The clastic grains mainly occur as point contacts (Fig. 4C), this shows that the precipitation time is early, cement content is higher and reservoir is tighter. The second type occurs as isolated calcite crystals filling some intergranular pores. The clastic grains usually have point-line contacts between each other, and

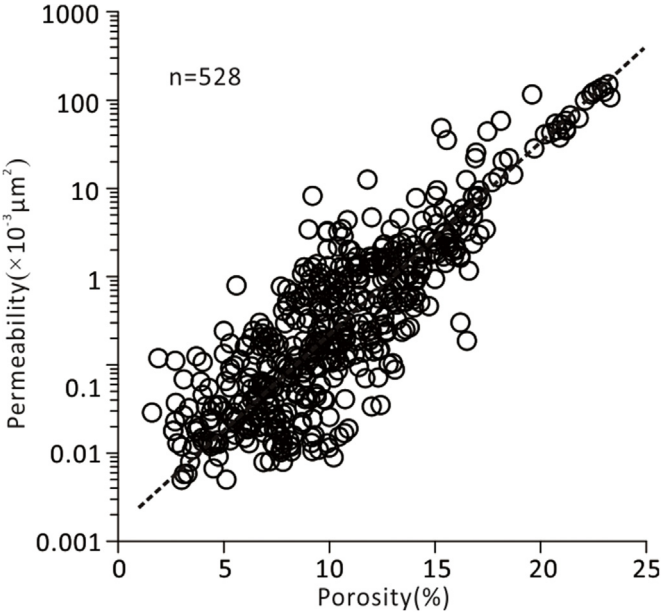

Fig. 6. Porosity vs. permeability plot for the beach-bar sandstone reservoirs from the Es4s unit in the Boxing Sag.

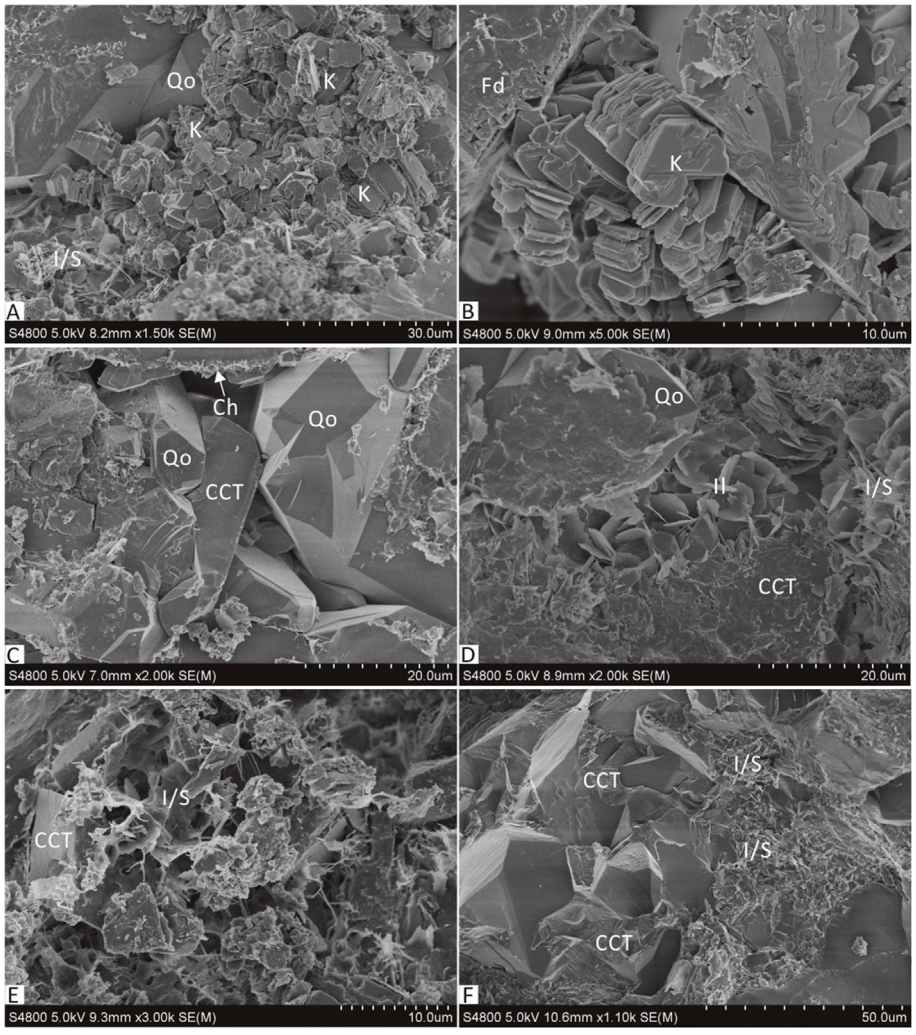

Fig. 5. Scanning electron microscope (SEM) images of beach-bar sandstones. (A) Quartz overgrowths, authigenic kaolinite and mixed-layer illite/smectite that fill pore spaces from well G890 at 2599.2 m; (B) Dissolution of feldspar and authigenic kaolinite that fills pore spaces from well G351 at 2434.24 m; (C) Carbonate cement and quartz overgrowths that fill pore spaces and authigenic chlorite that grows along the surface of detrital grains from well F151-1 at 2685.5 m; (D) Carbonate cement, quartz overgrowths, authigenic illite and mixed-layer illite/smectite that fill pore spaces from well F151-1 at 2701 m; (E) Carbonate cement and mixed-layer illite/smectite that fill pore spaces from well G890 at 2596.7 m; (F) Carbonate cement and mixed-layer illite/smectite that fill pore spaces from well G351 at 2464.79 m.

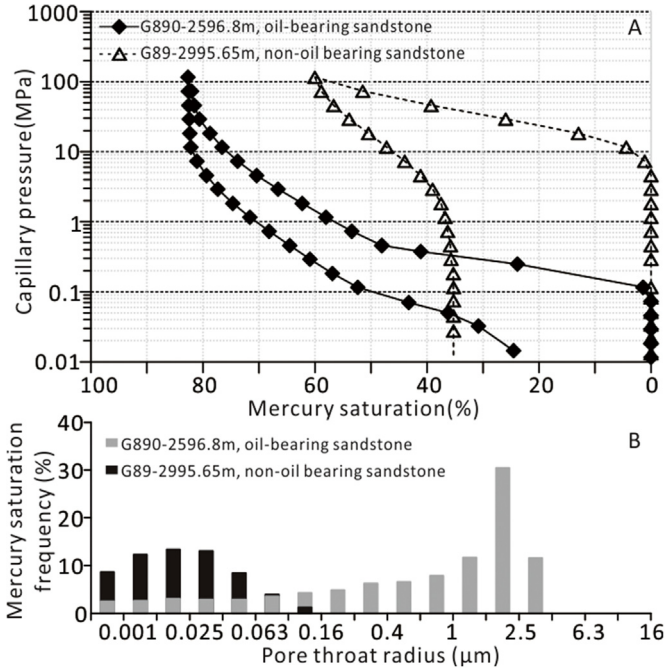

Fig. 7. Typical capillary pressure curves and the histograms of pore throat radii of oil-bearing and non-oil bearing beach-bar sandstones in the Boxing Sag.

cement content is relatively lower (Fig. 4D and E). The content of calcite in oil-bearing sandstones (0.5–13.3%, avg. 4.5%) is obviously lower than that of calcite in non-oil bearing sandstones (8–30.2%, avg. 14.2%) (Table 1). Dolomite and ankerite mainly occur as isolated crystals filling some intergranular pores (Fig. 4D and E). The contents of dolomite in oil-bearing sandstones and non-oil bearing sandstones have the similar characteristics as the contents of calcites (Table 1).

(3) Quartz Overgrowths: Authigenic quartz is usually formed as partial or whole overgrowth rims around quartz grains, with widths of 5–30 μm (Fig. 4A, E, F and Fig. 5A, C, D). The content of quartz overgrowths in oil-bearing sandstones is usually 0.4–3.5% volumetrically, with an average of 1.2%, which is higher than that of quartz overgrowths in non-oil bearing sandstones (Table 1).

(4) Matrix and Clay minerals: Clay minerals in the beach-bar sandstone mainly occur as matrix material and authigenic clay minerals. The content of clay minerals falls between 0 and 18%, with an average of 5.3%. The X-ray and SEM analyses indicate that the main components of the clays are kaolinite (Fig. 5A and B), chlorite (Fig. 5C), illite (Fig. 5D), and illite-smectite (I-S) mixed-layer minerals (Fig. 5A, D, E, and F). Kaolinite mainly occurs as pore-filling cement, occurring as well-crystallized, pseudohexagonal platelets and forms vermicular or booklet textures. The content of kaolinite in oil-bearing sandstones is higher than that of kaolinite in non-oil bearing sandstones (Table 1). Sheet-like illite mainly fills pores and the content in oil-bearing sandstones is lower than that in non-oil bearing sandstones (Table 1). Sheet-like or flake-like I-S mixed-layer clays mainly occur as pore-filling cement. Chlorite grows along the surfaces of detrital grains as rims. There is no obvious difference between the content of I-S mixed-layer clays and chlorite in oil-bearing and non-oil bearing sandstones (Table 1).

(5) Dissolution: Dissolution in the beach-bar sandstone reservoirs mainly occurred in feldspar and unstable rock fragments to form dissolution pores (Fig. 4G and H and Fig. 5B).

4.4. Reservoir pore types and properties

The beach-bar sandstone reservoirs have a positive relationship between porosity and permeability (Fig. 6). The porosity is usually between 1.6% and 23.3%, with an average of 10.4%; the permeability is usually 0.05×10^{-3} μm^2-152.3×10^{-3} μm^2, with an average of 4.8×10^{-3} μm^2.

The reservoir pore spaces of the beach-bar sandstones mainly occur as intergranular pores and dissolution pores in feldspars (Fig. 4A, D, E, F, G, H and Fig. 5B). The intergranular porosity (thin section estimation) in oil-bearing sandstones is usually between 4.5% and 17.2%, with an average of 6.6%; the intragranular porosity (thin section estimation) in oil-bearing sandstones is mainly between 0.5% and 2.8%, with an average of 0.9%. Both the intergranular porosity and intragranular porosity in oil-bearing sandstones are higher than those in non-oil bearing sandstones (Table 1). Fig. 7 shows two typical mercury

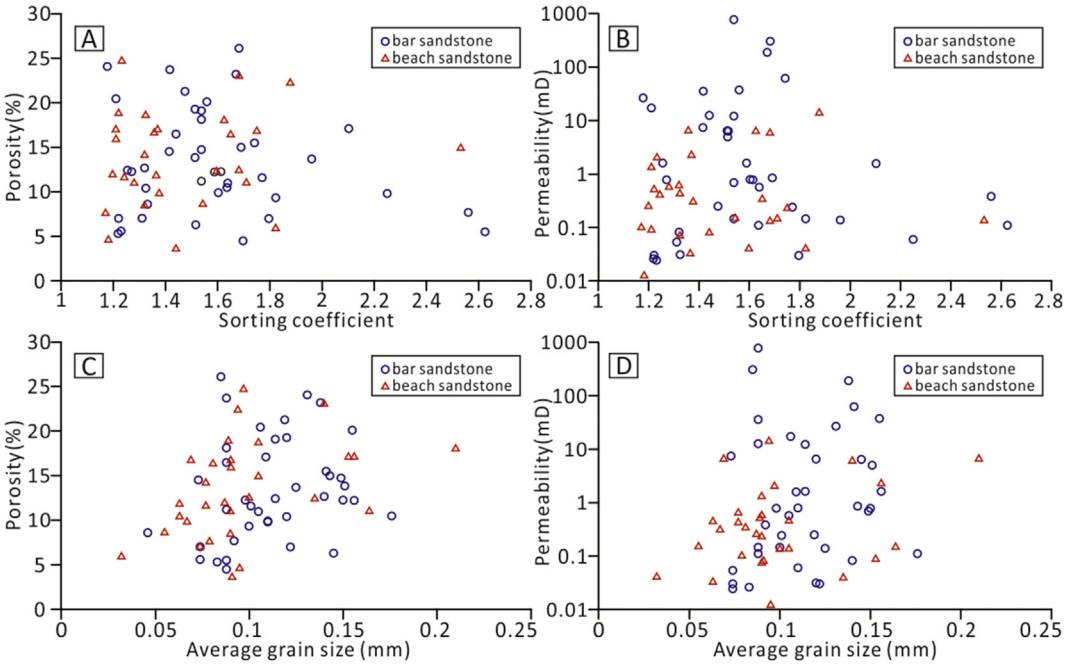

Fig. 8. Relationship between the sorting and grain size and the reservoir physical properties of the Eocene beach-bar sandstones in the Boxing Sag.

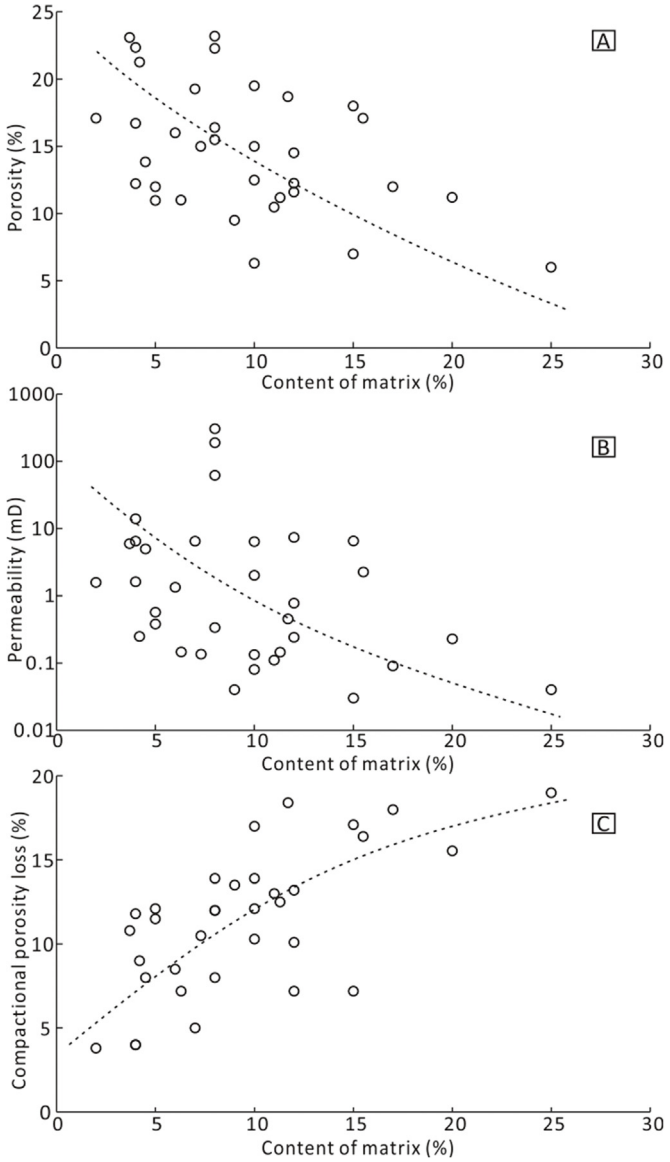

Fig. 9. Correlations between content of matrix and porosity, permeability and compactional porosity loss of beach-bar sandstones in the Boxing Sag.

injection curves for the oil-bearing sandstone and non-oil bearing sandstone. The displacement pressure and the pressure corresponding to a 50% Hg saturation of the oil-bearing sandstone (0.18 MPa, 0.74 MPa) are obviously lower than those of non-oil bearing sandstone (4.6 MPa, 73.5 MPa) (Fig. 7A). The pore throat radii of the oil-bearing sandstone sample are less than 4 μm, with an average of 1.3 μm, while the pore throat radii of the non-oil bearing sandstone sample are less than 0.16 μm, with an average of 0.03 μm (Fig. 7B).

4.5. Oil saturation of beach-bar sandstones

The oil saturations were tested from the core samples once they were removed from the ground by the Exploration and Development Research Institute of Shengli Oilfield. The test results show that the oil saturation of beach-bar sandstones is in the range of 6.5%–53.1% (avg. 27.1%).

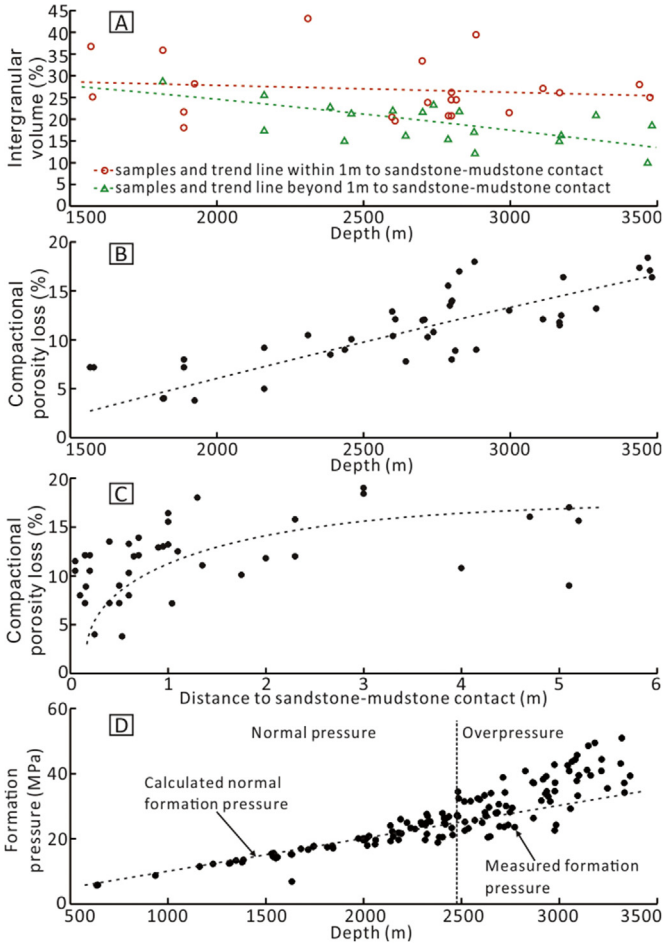

Fig. 10. (A) Correlation between intergranular volume and depth of beach-bar sandstones in the Boxing Sag. (B) Correlation between compactional porosity loss and depth of beach-bar sandstones in the Boxing Sag. (C) Correlation between compactional porosity loss and distance to sandstone-mudstone contact of beach-bar sandstones in the Boxing Sag. (D) Correlations between calculated normal formation pressure, measured formation pressure and depth in the Boxing Sag.

5. Discussion

5.1. Controls on reservoir quality

Reservoir quality is controlled by various factors, among which grain size, sorting, compaction, cementation and dissolution play more important roles (Rossi et al., 2002; Morad et al., 2010; Gaupp and Okkerman, 2011; Li et al., 2013). There are no obvious correlations of porosity and permeability with sorting coefficient and average grain size of beach sandstones or bar sandstones (Fig. 8), and almost no discrepancy of roundness cannot affect the reservoir petrophysical properties, which suggests that diagenetic factors controlled the reservoir quality during the burial process.

5.1.1. Compaction

The dominated point and line contacts and the deformed ductile grains (e.g., mica) indicates that compaction in beach-bar sandstones is mainly mechanical compaction (Fig. 4B). The initial porosity of the beach-bar sandstone is between 26.3% and 38.5% (avg. 32.6%) according to the Beard and Weyl's method (1973). The compactional porosity loss (COPL) during the burial process is 3.8%–19% (avg. 11.2%) as calculated using the Wang's method (Wang et al., 2017a), which is 17.3%–87.2% (avg. 57.3%) of the total porosity loss, indicating that mechanical compaction controlled the porosity reduction

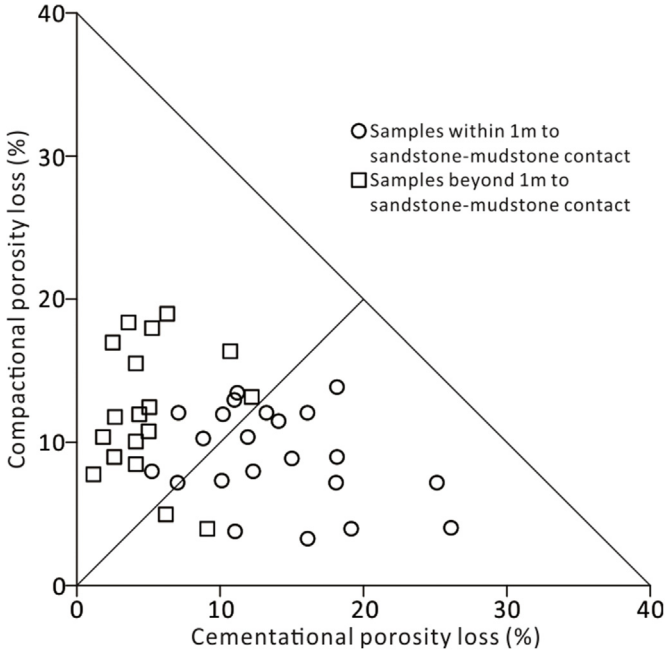

Fig. 11. Cross plot of compactional porosity loss versus cementational porosity loss for the beach-bar sandstones in the Boxing Sag.

in the beach-bar sandstones to a great extent.

Beach-bar sandstones contain certain content of matrix (including muddy matrix and clay matrix) (Table 1). Sandstones with a large amount of matrix have obviously low porosity and permeability and high compactional porosity loss (COPL) (Fig. 9). The deformation of plastic matrix can enhance the compaction degree to a great extent during the burial process (Gier et al., 2008; Van Den Bril and Swennen, 2009; Hammer et al., 2010; Dutton et al., 2012; Li et al., 2014).

The intergranular volume (IGV) has no obvious change with the increasing burial depth within 1 m to the sandstone-mudstone contact, whereas the IGV has a deceasing trend with the increasing burial depth beyond 1 m to the sandstone-mudstone contact (Fig. 10A). The COPL not only has an increasing trend with the increasing burial depth (Fig. 10B), but also increases gradually from the sandstone-mudstone contact to the center of sandstone (Fig. 10C). Within 1 m to the sandstone-mudstone contact, the COPL is relatively low and increases rapidly far away from the contact; beyond 1 m to the sandstone-mudstone contact, the COPLs is relatively high and tends to be stable (Fig. 10C). Carbonate or authigenic quartz cements filling intergranular pores can prevent compaction to some extent (Lima and De Ros, 2002; Li et al., 2014). It is clear from the IGV-Depth and COPL-CEPL diagrams (Lundegard, 1992) that the majority of samples within 1 m to the sandstone-mudstone contact have lost more porosity by cementation than by compaction, while the majority of samples beyond 1 m to the sandstone-mudstone contact have lost more porosity by compaction than by cementation (Figs. 10A and 11). The negative relationship between the COPL and cementational porosity loss (CEPL) indicates that cementation prevents compaction to some extent (Fig. 11).

Early overpressure is considered as an important factor that may prevent compaction to preserve porosity (Hansom and Lee, 2005; Madon, 2007). Overpressure occurs in beach-bar sandstone reservoirs with the depth below approximately 2500 m in the Boxing Sag (Fig. 10D), but the trend lines of the IGV beyond 1 m to sandstone-mudstone contact and COPL show no obvious change from shallow to deep (Fig. 10A and B). Fluid inclusion and basin numerical simulation analyses indicated that the overpressure of the Es4 interval in the Boxing Sag formed after 15 Ma B.P., which was mainly caused by hydrocarbon charge (Wang et al., 2017b). Rapidly COPL mainly occurs during the early diagenetic process (< 2000m) (Chen et al., 2009; Li et al., 2014). Thus, overpressure had little influence on compaction and porosity loss of the beach-bar sandstone reservoirs in the Boxing Sag.

5.1.2. Carbonate cementation

The cements in the beach-bar sandstone reservoirs in the Boxing Sag are dominated by carbonate, authigenic quartz and clay minerals (Figs. 4 and 5). Carbonate cement has the highest content and mainly fills primary intergranular pores and dissolution pores. The influence of the carbonate cements that fill the pores is much bigger than those cement that surround grains (e.g., quartz overgrowths) (Carvalho et al., 1995; Dutton, 2008; Morad et al., 2010). The carbonate cement content shows an obvious negative correlation with the porosity and permeability of the reservoirs (Fig. 12). Samples with high porosity and permeability usually have low content of carbonate cement. Therefore, the distribution of carbonate cements greatly controls the reservoir quality.

The samples in this study all have a certain amount of carbonate cements, with an extremely inhomogeneous distribution in the reservoirs. Only samples along the sandstone-mudstone contact have high carbonate cement content, where they exhibit tightly cemented natures. For instance, the carbonate cement contents from 3169.2 m to 3174 m in the sandstones near the sandstone-mudstone contacts in well F137 are usually high (avg. 20.2%), whereas the carbonate cement content in the middle of the sandstone is relatively low (avg. 9.6%) (Fig. 13). The porosity and permeability of sandstone near the sandstone-mudstone contact is very low (avg. 6.3% and 0.076×10^{-3} μm^2, respectively). However, the porosity and permeability in the middle of the sandstone is high (avg. 11.8% and 0.68×10^{-3} μm^2, respectively). Tightly carbonate-cemented sandstones are well-developed in the Eocene beach-bar sandbodies in the Boxing Sag.

According to the analytical test data of cores, the interbedded mudstones strongly affected the content of carbonate cement, porosity and permeability (Fig. 14). When the distance to the sandstone-mudstone contact is less than 1 m, the carbonate cement content is usually greater than 10%, and the porosity and permeability are less than 15% and 0.3×10^{-3} μm^2, respectively. When the distance to the sandstone-mudstone contact is more than 1 m, the content of carbonate cement is

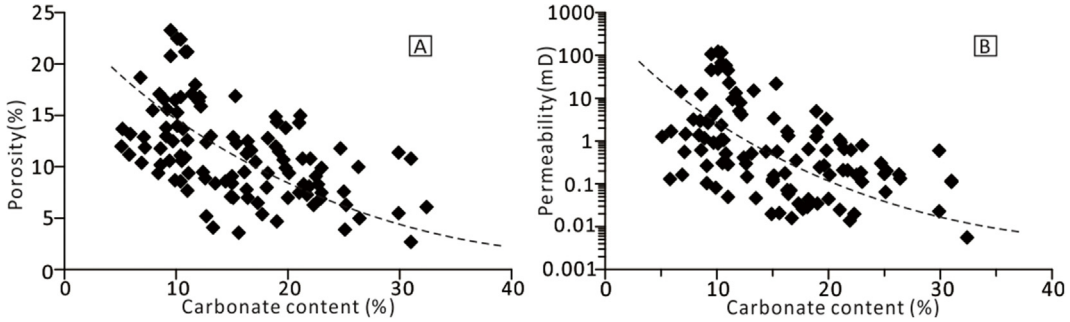

Fig. 12. Relationship between the carbonate cement content and the porosity and permeability of beach-bar sandstones from the Es4s unit in the Boxing Sag.

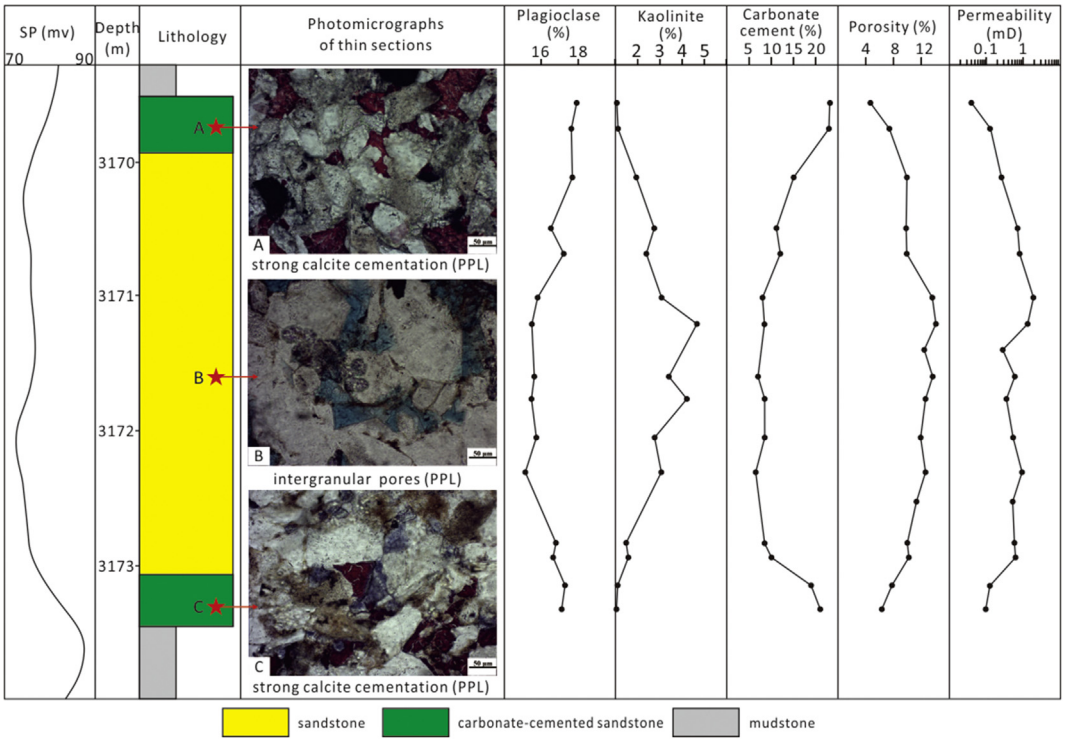

Fig. 13. Vertical distribution of plagioclase, kaolinite, carbonate cement, porosity and permeability in the interval of 3169.2 m–3174 m of Well F137 in the Boxing Sag.

low and decreases slowly with increasing distance to the contact, whereas the porosity and permeability increase slowly with the increasing distance to the contact. Hence, when the thickness of the sandstone is less than 1 m, it is usually tightly cemented by carbonate cements and the reservoir quality is very poor. When the thickness of the sandstone is greater than 1 m, the influence of carbonate cements on the middle part of the sandstone is weak and a large amount of intergranular pores can be preserved. Therefore, the thicker the sandstone, the weaker the influence of carbonate cement on the reservoir, and the better the reservoir quality (Li et al., 2014; Wang et al., 2017a).

According to the thin section observations, near the sandstone-mudstone contacts, carbonate cements fill the pores and mainly the point contact occurs between grains. In contrary, in the middle of the thick sandstones, the carbonate cements are mostly isolated crystals partly filling intergranular and dissolution pores (Fig. 13). The source of the carbonate cements in the clastic reservoirs is mainly external and internal (Dutton, 2008). The amount of carbonate rock fragments in the beach-bar sandstone is very low and insufficient to serve as the source for the carbonate cements. Due to the aforementioned distribution characteristics, the carbonate cements in the beach-bar sandstones are external and are most likely related to the diagenesis of the interbedding mudstones (Milliken and Land, 1993; Li et al., 2014; Wang et al., 2017a). Compositions of mudstones interbedded with beach-bar sandstones (Table 2) indicates that the source of the carbonate cements is mainly from the absorbed metal ions in the mudstones (Wang et al., 2018), the conversion of smectite to illite (Boles and Franks, 1979; McHargue and Price, 1982; Li et al., 2014), the K-feldspar dissolution and the corresponding conversion of kaolinite to illite in the mudstones (Macaulay et al., 1993; Li et al., 2014; Wang et al., 2017a). Compaction flow and diffusion are the two major ways for the mass transfer from mudstone to adjacent sandstone (Bjørlykke, 1993; Bjørlykke and Jahren, 2012), which broke the initial chemical balance and allowed the carbonate cements to form along the sandstone-mudstone contact (Milliken and Land, 1993; Dutton, 2008; Chen et al., 2009; Li et al., 2014; Wang et al., 2016, 2017a). A large number of metal ions were absorbed in the interbedded mudstones due to the high salinity lake water (Wang et al., 2015), promoting the transformation of clay minerals to release more ions, which facilitated early carbonate cementation along the sandstone-mudstone contact (Mansurbeg et al., 2008; Wang et al., 2013; Deconinck et al., 2014). The point contacts between grains also proved that the beach-bar sandstone reservoirs did not experience deep burial until the carbonate cements at the edge of the sandstone was precipitated (Wang et al., 2018). The negative relationship between COPL and CEPL also indicates that the early strong carbonate cementation can largely prevent compaction (Budd, 2002; Zhong et al., 2007; Morad et al., 2010), but the anti-compaction capacity in the middle of thick sandstone layers, where they show low carbonate cement content, is weak (Fig. 11).

5.1.3. Clay cementation

Clay is also an important factor that affects the reservoir quality (Li et al., 2014). The clay in the beach-bar sandstones mainly includes clay matrix and authigenic clay minerals that formed during diagenetic processes. During the burial process, the organic materials in the overlying hydrocarbon source rocks generated considerable organic acids. After these acids migrated into the reservoirs and reacted with feldspar and other unstable aluminosilicate components, numerous of dissolution pores and authigenic kaolinite were generated (Salem et al., 2005; Mansurbeg et al., 2008; Morad et al., 2010). For instance, the content of plagioclase in the sandstones near the sandstone-mudstone contact from 3169.2 m to 3174 m in well F137 is higher than that in the center of sandstones, while the content of kaolinite in sandstones near the sandstone-mudstone contact is lower than that in the center of sandstones (Fig. 13). During the burial process, the clay minerals generally experienced transformation from smectite and kaolinite to illite or chlorite. Different types of clay minerals have various effects on reservoir quality. The porosity and permeability of the beach-bar sandstones have a positive correlation with the kaolinite content (Fig. 15A and B) because the authigenic kaolinite indicates the development of dissolution pores in the feldspar (Fig. 13) and can have

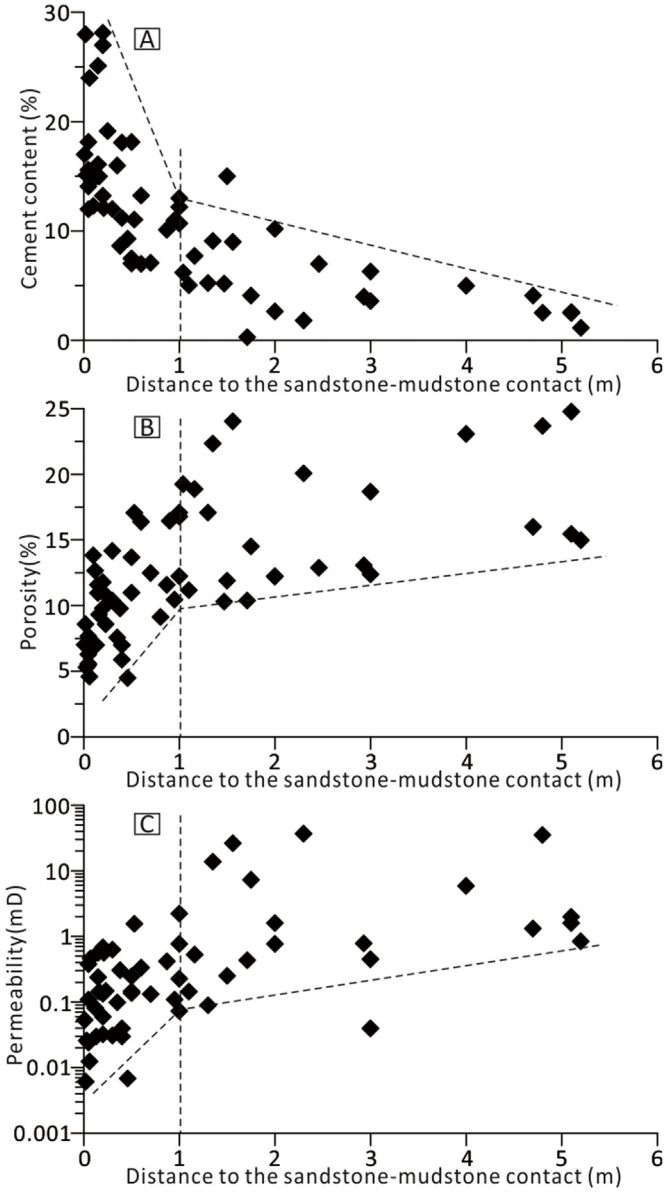

Fig. 14. Relationship between the content of carbonate cement, porosity, permeability and the distance from sandstone-mudstone contact.

numerous intercrystalline pores itself (Li et al., 2014), which can improve the porosity of the reservoirs (Morad et al., 2010; Li et al., 2014). Most illite filled the pore-throats in the beach-bar sandstones (Fig. 5A, D, E, F) and degraded the reservoir porosity and permeability. Thus, the porosity and permeability of the beach-bar sandstones have a negative correlation with the illite content (Fig. 15C and D). The porosity and permeability of the beach-bar sandstones also have negative relationships with the mixed-layer I-S content (Fig. 15E and F), suggesting that the mixed-layer I-S also fills reservoir pore spaces and reduces the reservoir quality. The grain-coating chlorite can prevent both compaction and the development of quartz overgrowths because of its oil-wet nature (Barclay and Worden, 2000), resulting in the preservation of intergranular pores (Thomson, 1982; Ehrenberg et al., 1993). The content of chlorite in beach-bar sandstones is very low (Table 1), the distribution of chlorite rims is very limited, and the thickness of chlorite rim is very small, which can only be seen under SEM (Fig. 5C). Due to the low chlorite content in the beach-bar sandstones, the thickness and development of the chlorite coats are not adequate to protect the reservoir quality (Fig. 15G and H).

5.1.4. Dissolution

Dissolution is a key factor that increases reservoir quality. Dissolution in the beach-bar sandstones mainly occurred in feldspar and other aluminosilicate components (Fig. 4G and H). The dissolution of unstable components (e.g., feldspar) requires a large amount of acidic formation fluids (Milliken, 1989; Wilkinson et al., 2001), mainly including meteoric water (Mansurbeg et al., 2006, 2012), pore water that contains organic acids and CO_2 (Schmidt and McDonald, 1979; Surdam et al., 1984; Morad et al., 2000; Mansurbeg et al., 2008) or deep thermal fluids (Taylor and Land, 1996). No evidence exists that describes the effects of deep thermal fluids in the study area and adjacent area (Li et al., 2014). Meteoric water is generally weakly acidic and unsaturated and is beneficial to strong carbonate and feldspar dissolution (Bjørlykke, 1984). The formation of authigenic kaolinite in reservoirs is often related to the incursion of meteoric water in shallow burial or epidiagenetic environments (Mansurbeg et al., 2006; 2012). Content of kaolinite in the shallow beach-bar sandstone reservoirs (< 2000m) is very low (Wang et al., 2017b), which suggests that the dissolution of feldspars and unstable rock fragments was probably nothing to do with meteoric water.

The beach-bar sandstones are adjacent to the overlying hydrocarbon source rock. The enormous organic acids and CO_2 that were produced by organic materials during the thermal evolution process mainly account for the dissolution of feldspar and other aluminosilicate components (Surdam et al., 1989). The products that were generated during the dissolution process of feldspar mainly include quartz and kaolinite (Rossel, 1982; Bjørlykke, 1998). The precipitation temperature of authigenic quartz in the beach-bar sandstones is usually 85°C-124 °C according to the fluid inclusion microthermometry (Wang et al., 2017b), which agrees with the favorable formation and preservation temperature of organic acids (80°C-120 °C) (Surdam et al., 1989). The geothermal gradient of the study area is 36.1 °C/km, and the average surface temperature is 20 °C (Qiu et al., 2004). Therefore, the depth range for the precipitation of authigenic quartz and dissolution of feldspar is approximately between 1800m and 2880 m, which is in accordance with the depth range of the maximum abundance of kaolinite (2000m-3200 m) (Wang et al., 2017b). Quartz overgrowths do not occur in samples with early diagenetic tight calcite cementation (Fig. 4C), in which the calcite was precipitated in the temperature range of 60°C–90 °C (Wang et al., 2016, 2017b). All of these indicate that the time for the dissolution of feldspar and formation of quartz overgrowths is later than that of early calcite cementation. Affected by the tightly cemented zones along the sandstone-mudstone contact of the thick sandstones, late pore fluids rich in organic acids and CO_2 were mainly concentrated in the middle of the thick sandstones, forming numerous dissolution pores in feldspar to increase the reservoir porosity and pore-throat size (Wang et al., 2017b). That is why the amount of dissolution pores has a positive relationship with the distance to the sandstone-mudstone contact (Fig. 16).

5.2. Diagenetic process and reservoir quality evolution

Analysis of diagenesis in beach-bar sandstones indicates that the diagenetic process and reservoir quality evolution in the edge of sandstones (less than 1 m to sandstone-mudstone contact) and in the center part of thick sandstones (beyond 1 m to sandstone-mudstone contact) are obviously different.

Influenced by the high-salinity depositional water, a large number of ions, such as Ca^{2+}, Mg^{2+}, Fe^{2+}, etc., were absorbed in mudstones (Milliken and Land, 1993; Li et al., 2014; Wang et al., 2018), which were transferred into the adjacent beach-bar sandstones by compaction flow during the early burial process (Bjørlykke, 1993; Bjørlykke and Jahren, 2012). These ions were concentrated in beach-bar sandstones along the sandstone-mudstone contact, forming strong calcite cementation (Fig. 17). Metal ions released by transformation of smectite to illite and chlorite in mudstones strengthened the calcite cementation

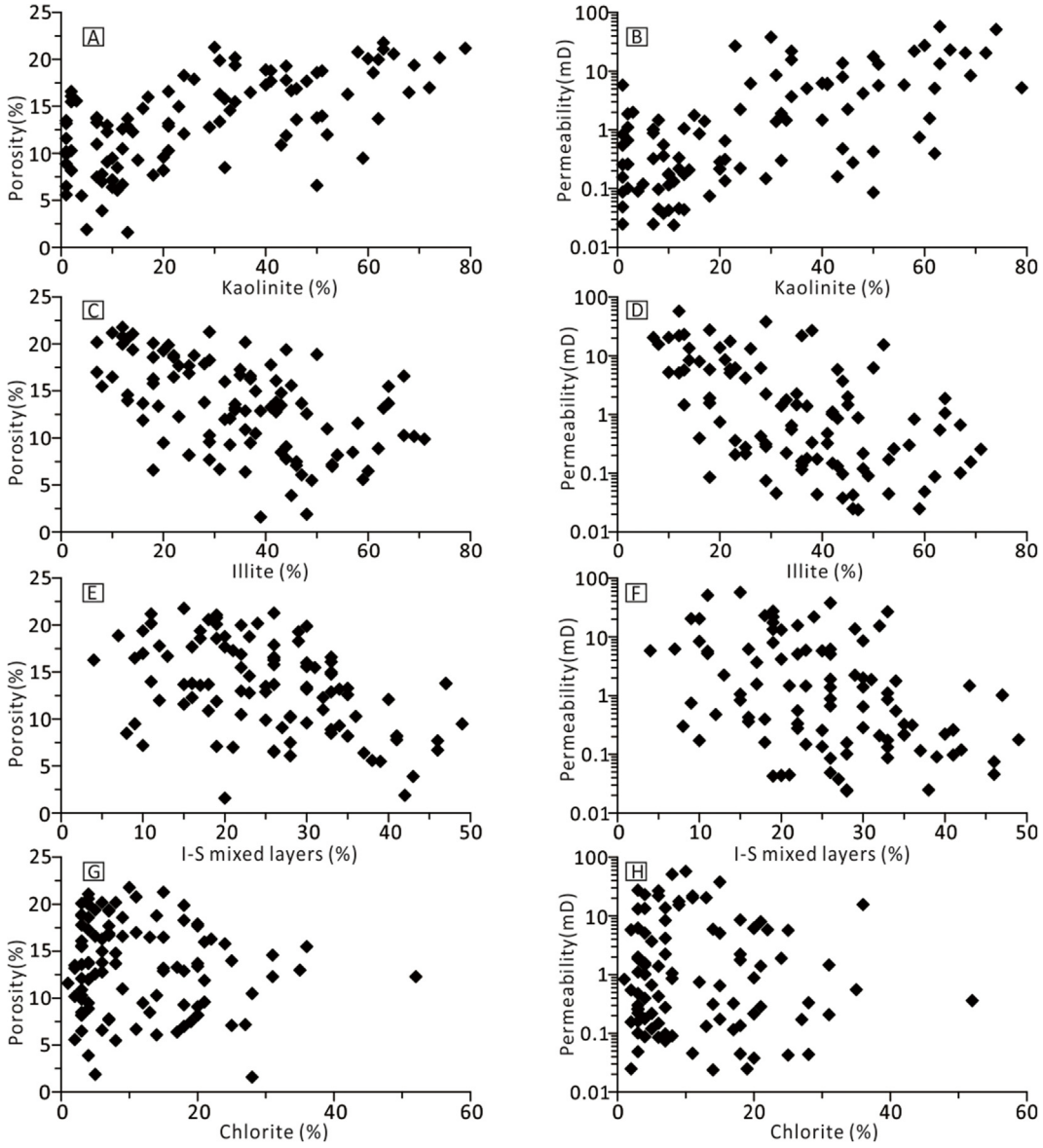

Fig. 15. Relationship between the reservoir quality and the relative content of clay minerals in beach-bar sandstones from the Es4s unit in the Boxing Sag.

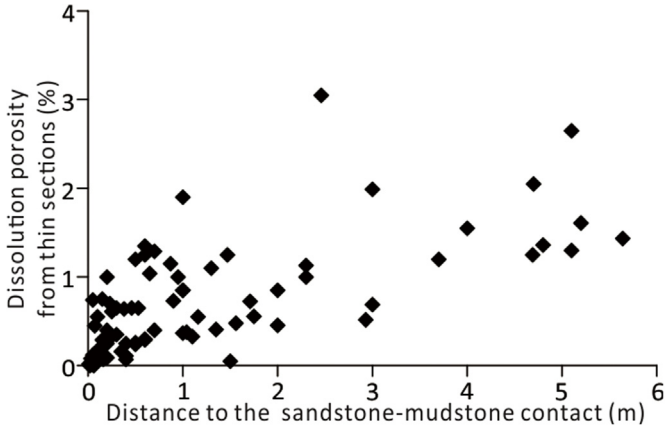

Fig. 16. Relationship between the dissolution porosity (from thin sections) and the distance to the sandstone-mudstone contact.

on the edge of beach-bar sandstones (Mansurbeg et al., 2008; Deconinck et al., 2014). Due to the relatively lower precipitation temperatures (60°C-90 °C) (Wang et al., 2016, 2017b), the precipitation time of calcites on the edge of sandstones were between 41.5Ma-35Ma (Fig. 17). Early strong calcite cementation restrained compaction on the edge of sandstones, which caused the rapid decrease of porosity and poor reservoir quality during the early burial process (Fig. 17). Late diagenesis was difficult to affect the reservoir porosity on the edge of sandstones due to the tight cementation.

The center part of thick sandstone was little affected by early calcite cementation, where the porosity was reduced by compaction in a great extent (Fig. 10A, C). The precipitation temperature of quartz overgrowth (85°C-124 °C) (Wang et al., 2017b) indicated that the dissolution of feldspar by organic acids and CO_2 and precipitation of authigenic quartz and kaolinite in the center part of sandstone were mainly during the time range of 38Ma-24.1Ma (Fig. 17). The precipitation temperature of isolated calcite and dolomite in the center part of sandstone ranged from 114 °C to 135 °C (Wang et al., 2017b), indicating the precipitation time range was 30.8Ma-8Ma (Fig. 17). The material source of late isolated calcite and dolomite was mainly from the dissolution of feldspar and transformation of clay minerals (Li et al., 2014; Wang et al., 2018). Porosity of the center part of sandstone has a trend of gradual decrease with the increasing burial depth affected by

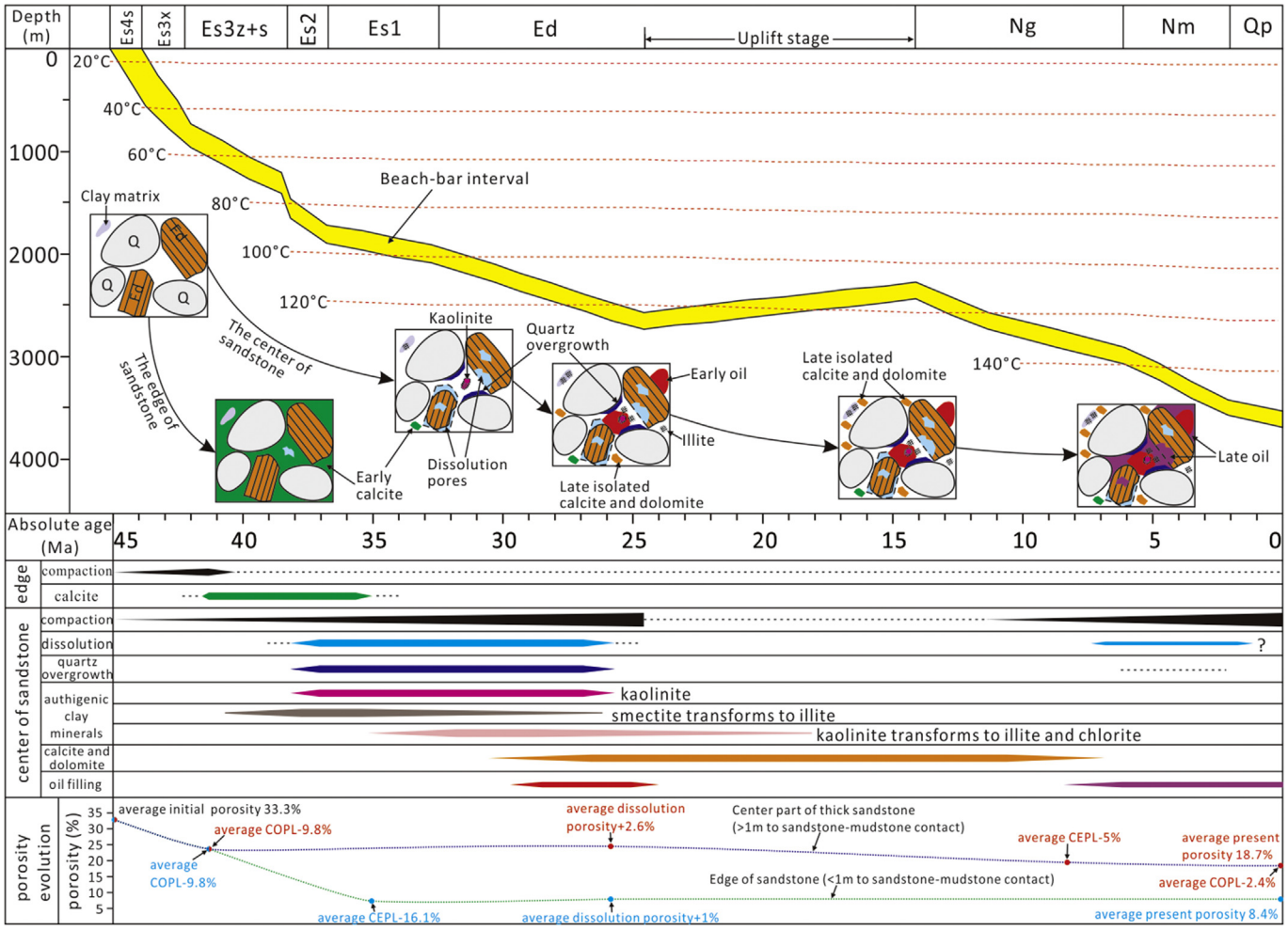

Fig. 17. Diagenetic process and reservoir porosity evolution of the beach-bar sandstones from the Es4s unit in the Boxing Sag. Temperatures were modeled by Hu et al. (2001) and burial history curves were modeled by Qiu et al. (2004).

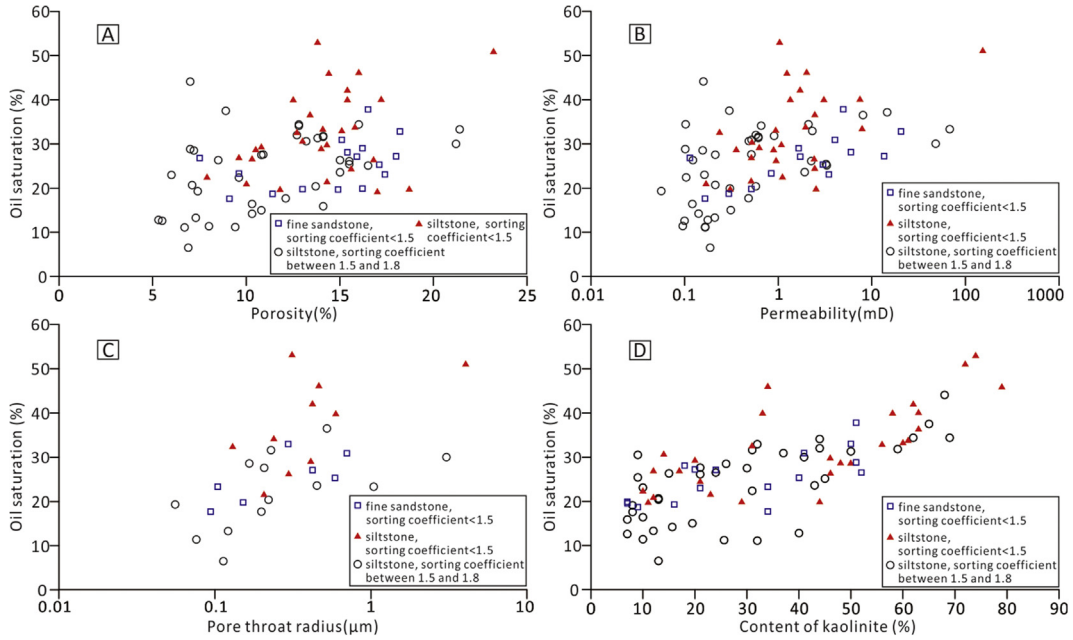

Fig. 18. Correlations of oil saturation with porosity (A), permeability (B), pore throat radius (C), and content of kaolinite (D) of the Eocene beach-bar fine sandstone and siltstone with different sorting coefficient in the Boxing Sag.

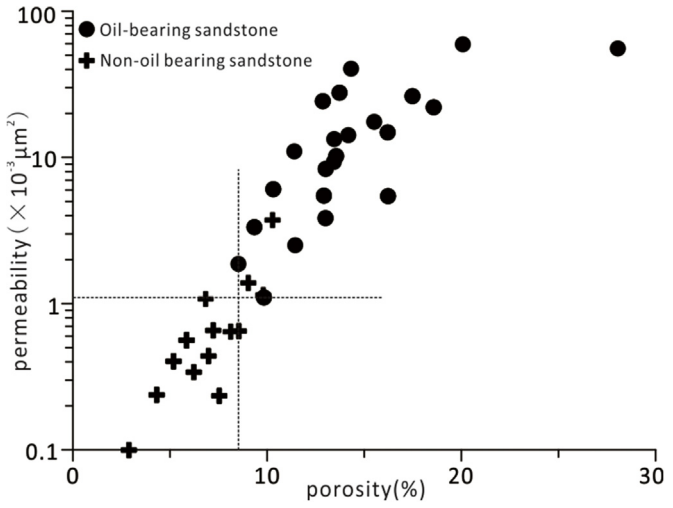

Fig. 19. Porosity and permeability of the oil-bearing and non-oil bearing samples. Samples were collected from the sealed cores for accurately determine the lower limits of porosity and permeability for hydrocarbon accumulation.

compaction. Influenced by feldspar dissolution, the porosity of the center part of sandstone was increased by feldspar dissolution pores to a certain extent (Fig. 17). Reservoir quality in the center part of sandstones is obviously better than that near the sandstone-mudstone contact.

5.3. Influences on hydrocarbon accumulation

Oiliness of the beach-bar sandstone reservoirs has a very strong heterogeneity. Oil saturation has obvious positive correlations with the porosity, permeability and pore-throat radius in fine sandstones and siltstones with different sorting coefficient (Fig. 18A, B, C), which suggests that hydrocarbon accumulation in beach-bar sandstone reservoirs is significantly controlled by reservoir petrophysical properties (Li et al., 2014). Porosity and pore-throat radius analyses indicate that the porosity of the oil-bearing sandstones is generally 6.3%–23.3% (avg. 13.5%) and their pore-throat radius is usually 0.33 μm-5.75 μm (avg. 1.63 μm), while the porosity of the non-oil bearing sandstone is generally 2.6%–16.6% (avg. 8.5%) and its pore-throat radius is 0.05 μm–0.73 μm (avg. 0.32 μm).

The dissolution of numerous unstable components occurred in the oil-bearing sandstones, such as the dissolution of feldspars. Under acidic water conditions, the dissolution of feldspar can form numerous dissolution pores, kaolinite and authigenic quartz (Rossel, 1982; Bjørlykke, 1998). Therefore, feldspar dissolution and kaolinization can form significant authigenic minerals and improve the reservoir's porosity and pore throat radius (Figs. 13 and 15A and B). Large pore-throat is conducive to the hydrocarbon entry and enhances accumulation in reservoirs because of the small resistance to fluid flow (Xi et al., 2016).

There were mainly two stages of hydrocarbon filling in the Eocene beach-bar sandstone reservoirs in the Boxing Sag according to the analysis of fluid inclusions, one was 29.5 Ma B.P.-24.1 Ma B.P., and the other one was after 8 Ma B.P. (Fig. 17; Wang et al., 2017b). The time of the first stage of hydrocarbon filling was later than that of the precipitation of the early diagenetic calcite near the sandstone-mudstone contact (Wang et al., 2017b), which caused the first stage of hydrocarbon to accumulate in the center part of the thick sandstones. After the early hydrocarbons filled the reservoirs, they greatly inhibited the carbonate cementation (Wilkinson et al., 2004; Gier et al., 2008), leading to the preservation of reservoir pore spaces. The average carbonate cement content in the oil-bearing sandstone is 8.5%, while the average carbonate cement content in the non-oil bearing sandstone is 18% (Table 1). On the other hand, the hydrocarbons tended to carry a large amount of organic acids into the reservoir during the filling process, promoting the dissolution of feldspar and other unstable components (Wilkinson et al., 2004). This is also the reason for the different rock compositions in the oil-bearing and non-oil bearing sandstones (Table 1). The pore-throat protected by the early hydrocarbon was also more conducive to the second stage of hydrocarbon filling. In addition, the hydrocarbon filling could change the hydrophilicity to lipophilicity of pore throat surface and promoted the second stage of hydrocarbon to accumulate in this type of reservoir spaces (Kumar et al., 2005). Kaolinite formed during the feldspar dissolution process could also enhanced the lipophilicity of pore-throat surface to promote the hydrocarbon accumulation (Fig. 18 D; Lebedeva and Fogden, 2011).

Because the reservoir's petrophysical properties are important factors that control hydrocarbon accumulation, a lower limit for the petrophysical properties defines the reservoir's ability to accumulate hydrocarbons. The porosity vs. permeability plot of oil-bearing and non-oil bearing sandstones indicates that the lower limit of the porosity and permeability for the oil-bearing sandstone reservoir is 8.5% and $1.02 \times 10^{-3}\,\mu m^2$, respectively (Fig. 19). Sandstones with petrophysical properties that are lower than the limit did not accumulate hydrocarbon.

6. Conclusions

The thickness of the single layer of beach-bar sandstone in the Boxing Sag is thin (usually 0.5–4.5 m) with fine grain size and medium to good sorting. The beach-bar sandstone reservoir experienced complicated diagenesis during the burial process, including mechanical compaction, carbonate cementation, quartz overgrowth cementation, clay cementation, feldspar and unstable rock fragment dissolution, etc. Because of the influence of compaction and selective and extensive cementation, the beach-bar sandstone reservoir has a very strong heterogeneity.

The mechanical compaction, carbonate cementation and dissolution are the main factors that control the petrophysical properties of the beach-bar sandstone reservoirs. Carbonate cements are mainly distributed along the sandstone-mudstone contacts. The early strong carbonate cementation can largely prevent compaction, but the anti-compaction capacity in the middle thick sandstones is poor. A weak carbonate cementation effect occurs in the middle part of the thick sandstones, but compaction occurred more intensely in the central part causing the destruction of primary pore spaces. Dissolution in the center part of thick sandstones increases the porosity and pore throat radius.

The analyses of the petrophysical properties and oil saturation suggest that a reservoir's petrophysical properties largely control hydrocarbon accumulation in beach-bar sandstones. Compared with non-oil bearing sandstones, oil-bearing sandstones have higher porosity and a larger pore-throat size. Sandstones with a porosity of less than 8.5% and/or low permeability of less than $1.02 \times 10^{-3}\,\mu m^2$ are mostly incapable of accumulating oil.

Acknowledgments

This work was co-funded by the National Nature Science Foundation of China (Grant No. U1762217), the Fundamental Research Funds for the Central Universities (18CX05027A, 16CX02027A), the National Science and Technology Special of China (2017ZX05009001), Strategic Priority Research Program of the Chinese Academy of Sciences (Grant No. XDA14010301), and the Scientific and Technological Innovation Project Financially Supported by Qingdao National Laboratory for Marine Science and Technology (No. 2015ASKJ01). Thanks are also expressed to the Geosciences Institute of the Shengli Oilfield, SINOPEC, for permission to access their in-house database, providing background geologic data and permission to

publish the results.

References

Aitken, A.E., Risk, M.J., Howard, J.D., 1988. Animal-sediment relationships on a sub-arctic intertidal flat, Pangnirtung Fiord, Baffin Island, Canada. J. Sediment. Res. 58, 969–978.

Barclay, S.A., Worden, R.H., 2000. Effects of reservoir wettability on quartz cementation in oil field. In: In: Worden, R.H., Morad, S. (Eds.), Clay Cements in Sandstones 29. IAS Special Publication, pp. 103–117.

Basilici, G., 1997. Sedimentary facies in an extensional and deep-lacustrine depositional system: the Pliocene Tiberino Basin. Central Italy. Sediment. Geol. 109, 73–94.

Beard, D.C., Weyl, P.K., 1973. Influence of texture on porosity and permeability of unconsolidated sand. AAPG Bull. 57, 349–369.

Bjørlykke, K., 1984. Formation of secondary porosity: how important is it? In: In: McDonald, D.A., Surdam, R.C. (Eds.), Clastic Diagenesis 37. AAPG Memoir, pp. 277–286.

Bjørlykke, K., 1993. Fluid flow in sedimentary basins. In: In: Cloetingh, S., Sassi, W., Horvath, F., Puigdefabregas, C. (Eds.), Basin Analysis and Dynamics of Sedimentary Basin Evolution 86. Sediment. Geol., pp. 137–158.

Bjørlykke, K., 1998. Clay mineral diagenesis in sedimentary basins-a key to the prediction of rock properties. Examples from North Sea Basin. Clay Miner. 33, 15–34.

Bjørlykke, K., Jahren, J., 2012. Open or closed geochemical systems during diagenesis in sedimentary basins: constraints on mass transfer during diagenesis and the prediction of porosity in sandstone and carbonate reservoirs. AAPG Bull. 96, 2193–2214.

Boles, J.R., Franks, S.G., 1979. Clay diagenesis in Wilcox sandstones of southwest Texas: implications of smectite diagenesis on sandstone cementation. J. Sediment. Petrol. 49, 55–70.

Budd, D.A., 2002. The relative roles of compaction and early cementation in the destruction of permeability in carbonate grainstones: a case study from the Paleogene of west-central Florida, USA. J. Sediment. Res. 72, 116–128.

Cao, Y., Wang, J., Liu, H., 2010. Preliminary study on the hydrodynamic mechanism of beach-bar sandbodies with environmentally sensitive grain size components——an example for beach-bar sandbodies sediments of the upper part of the fourth member of the Shahejie Formation in the western dongying depression. Acta Sedimentol. Sin. 28, 274–284 in Chinese with English abstract.

Carvalho, M.V.F., De Ros, L.F., Gomes, N.S., 1995. Carbonate cementation patterns and diagenetic reservoir facies in the Campos Basin Cretaceous turbidites, offshore eastern Brazil. Mar. Petrol. Geol. 12, 741–758.

Chen, D., Pang, X., Jiang, Z., Zeng, J., Qiu, N., Li, M., 2009. Reservoir characteristics and their effects on hydrocarbon accumulation in lacustrine turbidites in the Jiyang Super-depression, Bohai Bay Basin, China. Mar. Petrol. Geol. 26, 149–162.

Deconinck, J.F., Crasquin, S., Bruneau, L., Pellenard, P., Baudin, F., Feng, Q., 2014. Diagenesis of clay minerals and K-bentonites in late Permian/early triassic sediments of the sichuan basin (chaotian section, Central China). J. Asian Earth Sci. 81, 28–37.

Deng, H., Xiao, Y., Ma, L., Jiang, Z., 2011. Genetic type, distribution patterns and controlling factors of beach and bars in the second member of the Shahejie Formation in the dawangbei sag, Bohai Bay, China. Geol. J. 46, 380–389.

Dutton, S.P., 2008. Calcite cement in Permian deep-water sandstones, Delaware Basin west Texas: origin, distribution, and effect on reservoir properties. AAPG Bull. 92, 765–787.

Dutton, S.P., Loucks, R.G., Day-Stirrat, R.J., 2012. Impact of regional variation in detrital mineral composition on reservoir quality in deep to ultradeep lower Miocene sandstones, western Gulf of Mexico. Mar. Petrol. Geol. 35, 139–153.

Ehrenberg, S.N., Aagaard, P., Wilson, M.J., Fraser, A.R., Duthie, D.M., 1993. Depth dependent transformation of kaolinite to dickite in sandstones of the Norwegian Continental Shelf. Clay Miner. 28, 325–352.

Engels, S., Roberts, M.C., 2005. The architecture of prograding sandy-gravel beach ridges formed during the last Holocene highstand: southwestern British Columbia, Canada. J. Sediment. Res. 75, 1052–1064.

Fisher, T.G., 2005. Strandline analysis in the southern basin of glacial lake agassiz, Minnesota and north and south Dakota, USA. Geol. Soc. Am. Bull. 117, 1481–1496.

Folk, R.L., 1980. Petrology of Sedimentary Rocks. Hemphill Publishing, Austin, Texas, pp. 182.

Gao, X., Deng, H., Lin, H., 2014. Stratigraphic controls on the evolution and distribution of lacustrine beach and bar Sands-Bohai Bay basin in China. Manuf. Eng. Environ. Eng. 84, 1513–1519.

Gaupp, R., Okkerman, J.A., 2011. Diagenesis and reservoir quality of Rotliegend sandstones in the Northern Netherlands-a review. In: Grotsch, J., Gaupp, R. (Eds.), Permian Rotliegend of the Netherlands. Soc. Sediment. Geol. Spec. Pub., pp. 193–226.

Gier, S., Worden, R.H., Johns, W.D., Kurzweil, H., 2008. Diagenesis and reservoir quality of miocene sandstones in the Vienna basin, Austria. Mar. Petrol. Geol. 25, 681–695.

Goulart, E.S., Calliari, L.J., 2013. Medium-term morphodynamic behavior of a multiple sand bar beach. J. Coast Res. 65, 1774–1779.

Guo, X., He, S., Liu, K., Song, G., Wang, X., Shi, Z., 2010. Oil generation as the dominant overpressure mechanism in the cenozoic dongying depression, Bohai Bay Basin, China. AAPG Bull. 94, 1859–1881.

Guo, S., Tan, L., Lin, C., Li, H., Lu, X., Wang, H., 2014. Hydrocarbon accumulation characteristics of beach-bar sandstones in the southern slope of the dongying sag, Jiyang depression, Bohai Bay Basin, China. Petrol. Sci. 11, 220–233.

Hammer, E., Mork, M.B.E., Naess, A., 2010. Facies controls on the distribution of diagenesis and compaction in fluvial-deltaic deposits. Mar. Petrol. Geol. 27, 1737–1751.

Han, H., 2009. Research on the characteristics of thin-alternating-bed seismic waveform-A case study of the beach bar sandstones of Es4 in Boxing Sag. Earth Sci. Front. 16, 349–355 in Chinese with English abstract.

Hansom, J., Lee, M.K., 2005. Effects of hydrocarbon generation, basal heat flow and sediment compaction on overpressure development: a numerical study. Petrol. Geosci. 11, 353–360.

Hu, S., O'Sullivan, P.B., Raza, A., Kohn, B.P., 2001. Thermal history and tectonic subsidence of the Bohai Basin, northern China: a Cenozoic rifted and local pull-apart basin. Phys. Earth Planet. In. 126, 221–235.

Ji, Y., Lu, H., Liu, Y., 2013. Sedimentary model of shallow water delta and beach bar in the member 1 of Paleogene funing formation in Gaoyou sag, Subei Basin. J. Palaeogeogr. 15 (5), 729–740 in Chinese with English abstract.

Jiang, Z., Liu, H., Zhang, S., Su, X., Jiang, Z., 2011. Sedimentary characteristics of large-scale lacustrine beach-bars and their formation in the Eocene Boxing sag of Bohai Bay Basin, east China. Sedimentology 58, 1087–1112.

Kumar, K., Dao, E., Mohanty, K.K., 2005. AFM study of mineral wettability with reservoir oils. J. Colloid Interface Sci. 289, 206–217.

Lampe, C., Song, G., Cong, L., Mu, X., 2012. Fault control on hydrocarbon migration and accumulation in the Tertiary Dongying depression, Bohai Basin, China. AAPG Bull. 96, 983–1000.

Lebedeva, E.V., Fogden, A., 2011. Wettability alteration of kaolinite exposed to crude oil in salt solutions. Colloid. Surface. Physicochem. Eng. Aspect. 377, 115–122.

Li, D., Dong, C., Lin, C., Ren, L., Jiang, T., Tang, Z., 2013. Control factors on tight sandstone reservoirs below source rocks in the Rangzijing slope zone of southern Songliao Basin, East China. Petrol. Explor. Dev. 40, 742–750.

Li, Q., Jiang, Z., Liu, K., Zhang, C., You, X., 2014. Factors controlling reservoir properties and hydrocarbon accumulation of lacustrine deep-water turbidites in the Huimin Depression, Bohai Bay Basin, East China. Mar. Petrol. Geol. 57, 327–344.

Lima, R.D., De Ros, L.F., 2002. The role of depositional setting and diagenesis on the reservoir quality of Devonian sandstones from the Solimoes Basin, Brazilian Amazonia. Mar. Petrol. Geol. 19, 1047–1071.

Liu, Q., Zhu, H., Shu, Y., Zhu, X., Yang, X., Fu, X., 2015. Provenance systems and their control on the beach-bar of Paleogene enping formation, enping sag, Pearl River Mouth Basin. Acta Petrol. Sin. 36 (3), 286–299 in Chinese with English abstract.

Lundegard, P.D., 1992. Sandstone porosity loss-a "big picture" view of the importance of compaction. J. Sediment. Petrol. 62, 250–260.

Macaulay, C.I., Haszeldine, R.S., Fallick, A.E., 1993. Distribution, chemistry, isotopic composition and origin of diagenetic carbonates: magnus Sandstone, North Sea. J. Sediment. Res. 63, 33–43.

Madon, M., 2007. Overpressure development in rift basins: an example from the Malay Basin, offshore Peninsular Malaysia. Petrol. Geosci. 13, 169–180.

Mansurbeg, H., El-ghali, M.A.K., Morad, S., Plink-Bjoklund, P., 2006. The impact of meteoric water on the diagenetic alterations in deep-water, marine siliciclastic turbidites. J. Geochem. Explor. 89 (1–3), 254–258.

Mansurbeg, H., Morad, S., Salem, A., Marfil, R., El-ghali, M.A.K., Nystuen, J.P., Caja, M.A., Amorosi, A., Garcia, D., La Iglesia, A., 2008. Diagenesis and reservoir quality evolution of palaeocene deep-water, marine sandstones, the Shetland-Faroes Basin, British continental shelf. Mar. Petrol. Geol. 25, 514–543.

Mansurbeg, H., De Ros, L.F., Morad, S., Ketzer, J.M., El-Ghali, M.A.K., Caja, M.A., Othman, R., 2012. Meteoric-water diagenesis in late Cretaceous canyon-fill turbidite reservoirs from the Espirito Santo Basin, eastern Brazil. Mar. Petrol. Geol. 37, 7–26.

McHargue, T.R., Price, R.C., 1982. Dolomite from clay in argillaceous limestones or shale associated marine carbonates. J. Sediment. Petrol. 52, 873–886.

Milliken, K.L., 1989. Petrography and composition of authigenic feldspars, oligocene Frio formation, south Texas. J. Sediment. Petrol. 59 (3), 361–374.

Milliken, K.L., Land, L.S., 1993. The origin and fate of silt sized carbonate in subsurface Miocenee Oligocene mudstones, south Texas Gulf Coast. Sedimentology 40, 107–124.

Monroe, S., 1981. Late oligocene-early miocene facies and lacustrine sedimentation, upper ruby river basin, southwestern Montana. J. Sediment. Petrol. 51, 0939–0951.

Morad, S., Ketzer, J.M., De Ros, L.F., 2000. Spatial and temporal distribution of diagenetic alterations in siliciclastic rocks: implications for mass transfer in sedimentary basins. Sedimentology 47 (s1) 95–20.

Morad, S., Al-Ramadan, K., Ketzer, J.M., De Ros, L.F., 2010. The impact of diagenesis on the heterogeneity of sandstone reservoirs: a review of the role of depositional facies and sequence stratigraphy. AAPG Bull. 94, 1267–1309.

Patel, S.J., Desai, B.G., Bhatt, N.Y., 2002. Origin of air trap structures in beach-bar complex and their significance - a study from Mandvi coast, Gulf of Kachchh, Western India. J. Geol. Soc. India 60, 391–399.

Qiu, N., Li, S., Zeng, J., 2004. Thermal history and tectonic-thermal evolution of the Jiyang depression in the Bohai Bay Basin, east China. Acta Geol. Sin. 78, 263–269 in Chinese with English abstract.

Reid, I., Frostick, L.E., 1985. Beach orientation, bar morphology and the concentration of metalliferous placer deposits: a case study, Lake Turkana, N Kenya. J. Geol. Soc. 142, 837–848.

Rossel, N.C., 1982. Clay mineral diagenesis in roliegend aeolian sandstones of the southern north sea. Clay Miner. 17, 69–77.

Rossi, C., Kalin, O., Arribas, J., Tortosa, A., 2002. Diagenesis, provenance and reservoir quality of triassic TAGI sandstones from ourhoud field, Berkine (Ghadames) basin, Algeria. Mar. Petrol. Geol. 19, 117–142.

Salem, A.M., Ketzer, J.M., Morad, S., Rizk, R.R., Al-Aasm, I.S., 2005. Diagenesis and reservoir-quality evolution of incised-valley sandstones: evidence from the abu madi gas reservoirs (upper miocene), the nile delta basin, Egypt. J. Sediment. Res. 75, 572–584.

Schmidt, V., McDonald, D.A., 1979. Textures and recognition of secondary porosity in sandstones. In: In: Scholle, P.A., Schluger, P.R. (Eds.), Aspects of Diagenesis 26. SEPM Special Publication, pp. 209–225.

Si, X., Xie, J., Zhang, J., 2007. The mechanism of secondary pore of the beach-bar sandstones and prediction of favorable regions in the upper Es4 of the Palaeogene.

Boxing Sag. J. China Univ. Geosci. 18, 302–304 in Chinese with English abstract.
Surdam, R.C., Boese, S.W., Crossey, L.J., 1984. The chemistry of secondary porosity. In: In: Surdam, R.C., McDonald, D.A. (Eds.), Clastic Diagenesis 37. AAPG Memoir, pp. 127–149.
Surdam, R.C., Dunn, T.L., Heasler, H.P., Macgowan, D.B., 1989. Porosity evolution in sandstone/shale systems. In: Hutcheon, I.E. (Ed.), Short Course on Burial Diagenesis. Mineralogical Association of Canada, pp. 61–134.
Taylor, T.R., Land, L.S., 1996. Association of an allochthonous waters and reservoir enhancement in deeply buried Miocene sandstones: Picaroon Field, Corsair Trend, Offshore Texas. In: In: Crossey, L.J., Loucks, R., Totten, M.W. (Eds.), Siliciclastic Diagenesis and Fluid Flow: Concepts and Applications 55. SPEM Special Publication, pp. 37–48.
Thomson, A., 1982. Preservation of porosity in the deep Woodbine/Tuscaloosa trend, Louisiana. J. Petrol. Technol. 34, 1156–1162.
Tian, J., Jiang, Z., 2012. Comparison and analysis of beach bars sedimentary characteristics of upper Es4 in huimin and dongying depression. J. Jilin Univ. Earth Sci. Ed. 42, 612–623 in Chinese with English abstract.
Udden, J.A., 1914. Mechanical composition of clastic sediments. GSA Bull 25, 655–744.
Van Den Bril, K., Swennen, R., 2009. Sedimentological control on carbonate cementation in the Luxembourg sandstone formation. Geol. Belg. 12, 3–23.
Wang, J., Cao, Y., Gao, Y., Liu, J., 2013. Diagenetic characteristics and formation mechanism of red beds reservoirs of Paleogene in Dongying depression. Acta Petrol. Sin. 34, 283–292 in Chinese with English abstract.
Wang, J., Cao, Y., Liu, H., Gao, Y., 2015. Formation conditions and sedimentary model of over-Flooding lake deltas within continental lake basins: an example from the Paleogene in the Jiyang subbasin, Bohai Bay Basin. Acta Geol. Sin. 89, 270–284.
Wang, J., Cao, Y., Liu, K., Liu, J., Xue, X., Xu, Q., 2016. Pore fluid evolution, distribution and water-rock interactions of carbonate cements in red-bed sandstone reservoirs in the Dongying Depression, China. Mar. Petrol. Geol. 72, 279–294.
Wang, J., Cao, Y., Liu, K., Liu, J., Muhammad, K., 2017a. Identification of sedimentary-diagenetic facies and reservoir porosity and permeability prediction: an example from the Eocene beach-bar sandstone in the Dongying Depression, China. Mar. Petrol. Geol. 82, 69–84.
Wang, J., Cao, Y., Song, G., Liu, H., 2017b. Diagenetic evolution and formation mechanisms of high-quality reservoirs under multiple diagenetic environmental constraints: an example from the Paleogene beach-bar sandstone reservoirs in the dongying depression, Bohai Bay Basin. Acta Geol. Sin. 91, 232–248.
Wang, J., Cao, Y., Liu, K., Costanzo, A., Feely, M., 2018. Diagenesis and evolution of the lower Eocene red-bed sandstone reservoirs in the Dongying Depression, China. Mar. Petrol. Geol. 94, 230–245.
Wentworth, C.K., 1922. A scale of grade and class terms for clastic sediments. J. Geol. 30, 377–392.
Wilkinson, M., Milliken, K.L., Haszeldine, R.S., 2001. Systematic destruction of K-feldspars in deeply buried rift and passive margin sandstones. J. Geol. Soc. 158, 675–683.
Wilkinson, M., Haszeldine, R.S., Ellam, R.M., Fallick, A., 2004. Hydrocarbon filling history from diagenetic evidence: Brent Group, UK north sea. Mar. Petrol. Geol. 21 (4), 443–455.
Williams, J.J., Conner, D.C., Peterson, K.E., 1975. Piper oil field, North Sea; fault-block structure with upper Jurassic beach/bar reservoir sands. AAPG Bull. 59, 158–1601.
Xi, K., Cao, Y., Haile, B.G., Zhu, R., Jaren, J., Bjørlykke, K., Hellevang, H., 2016. How does the pore-throat size control the reservoir quality and oiliness of tight sandstones? The case of the Lower Cretaceous Quantou Formation in the southern Songliao Basin, China. Mar. Petrol. Geol. 76, 1–15.
Yuan, X., Qiao, H., 2002. Exploration of subtle reservoir in prolific depression of Bohai Bay basin. Oil Gas Geol. 23, 130–133 in Chinese with English abstract.
Zhang, H., Liu, Q., Zhang, L., Zhang, J., 2005. Lacustrine basin evolution and favorable sedimentary facies belt for source rocks abounding in the Shahejie Formation of Paleogene in Dongying Sag, Shandong Province. J. Palaeogeogr. 7, 383–397 in Chinese with English abstract.
Zhao, D., Zhu, X., Dong, Y., Wu, D., Zhu, M., 2014. Application of seismic sedimentology to prediction of beach and bar sandbodies in gentle slope of lacustrine basin: a case study of the Lower Cretaceous in Chepaizi area, Junggar Basin, NW China. Petrol. Explor. Dev. 41, 60–67.
Zhao, X., Wang, Q., Jin, F., Luo, N., Fan, B., Li, X., Qin, F., Zhang, H., 2015. Re-exploration program for petroleum-rich sags and its significance in Bohai Bay Basin, East China. Petrol. Explor. Dev. 42 (6), 723–733.
Zhong, D., Zhu, X., Li, S., Xie, N., 2007. Influence of early carbonate cementation on the evolution of sandstones: a case study from Silurian sandstones of Manjiaer depression, Tarim basin. Acta Sedimentol. Sin. 25, 885–890 in Chinese with English abstract.